CD103 integrin identifies a high IL-10-producing FoxP3^{+} regulatory T cell population suppressing allergic airway inflammation

Sofia Tagkareli,[1] Maria Salagianni,[1] Ioanna Galani,[1] Maria Manioudaki,[1] Eleftherios Pavlos,[1] Kalliopi Thanopoulou,[1] and Evangelos Andreakos[1,2 *]

[1] Laboratory of Immunobiology, Center for Clinical, Experimental Surgery and Translational Research, Biomedical Research Foundation of the Academy of Athens, Athens, Greece

[2] Airway Disease Infection Section, National Heart and Lung Institute, Imperial College London, London W2 1NY, United Kingdom

[*] Corresponding author, e.mail: vandreakos@bioacademy.gr

Abstract

Background: Although FoxP3^{+} regulatory T (Treg) cells constitute a highly heterogeneous population, with different regulatory potential depending on the context, distinct subsets or phenotypes remain poorly defined. This hampers the development of immunotherapy for allergic and autoimmune disorders. This study aimed at characterizing distinct FoxP3^{+} Treg subpopulations involved in the suppression of Th2-mediated allergic inflammation in the lung.

Methods: We used an established mouse model of allergic airway disease based on ovalbumin sensitization and challenge to analyze FoxP3^{+} Tregs during the induction and resolution of inflammation, and identify markers that distinguish their most suppressive phenotypes. We also developed a new knock-in mouse model (*Foxp3^{cre}Cd103^{dtr}*) enabling the specific ablation of CD103^{+}FoxP3^{+} Tregs for functional studies.

Results: We found that during resolution of allergic airway inflammation in mice >50% of FoxP3$^+$ Treg cells expressed the integrin CD103 which marks FoxP3$^+$ Treg cells of high IL-10 production, increased expression of immunoregulatory molecules such as KLRG1, ICOS and CD127, and enhanced suppressive capacity for Th2-mediated inflammatory responses. CD103$^+$FoxP3$^+$ Tregs were essential for keeping allergic inflammation under control as their specific depletion in *Foxp3^{cre}Cd103^{dtr}* mice lead to severe alveocapillary damage and eosinophilic pneumonia, markedly reducing the lifespan of the experimental animals. Conversely, adoptive transfer of CD103$^+$FoxP3$^+$ Tregs effectively treated disease, attenuating Th2 responses and allergic inflammation in an IL-10-dependent manner.

Conclusion: Our study identifies a novel regulatory T cell population, defined by CD103 expression, programmed to prevent exuberant type 2 inflammation and keep homeostasis in the respiratory tract under control. This has important therapeutic implications.

Key words: airway inflammation, allergy, CD103, regulatory T cells, T cells

Introduction

Regulatory T cells (Tregs) constitute a special subset of the T lymphocyte population with a crucial role in the maintenance of peripheral tolerance[1]. Tregs maintain immune homeostasis [2], prevent autoimmunity[3] and regulate inflammation induced by pathogens and other environmental insults[4,5]. Besides their highly beneficial role in preventing autoimmune and chronic inflammatory diseases, they also block pivotal responses by suppressing sterile immunity to certain pathogens and limiting anti-tumor immunity[6]. They originate in the thymus (natural Tregs, nTregs)[7] or can develop in the periphery from naïve T cells following appropriate cytokine signals (induced Tregs, iTregs)[8,9], and are all defined by the expression of transcription factor FoxP3 (Forkhead box P3). FoxP3 has an imperative role in the differentiation, maintenance and functional activities of Tregs[10]. FoxP3 deficiency or suboptimal expression, both in humans and mice, induces a severe systemic inflammatory phenotype such as autoimmunity, colitis and allergic response[11,12].

Recent studies have revealed that not all Tregs are the same but rather constitute a heterogeneous population with high complexity. They express different transcription factors, immune checkpoint receptors and cytokines depending on the inflammatory environment and the type of T helper cell responses that need regulation[13]. Moreover, they can alter their migratory, functional and homeostatic properties by up-regulating cell surface molecules, receptors, cytokines and chemokines. In a Th1 inflammatory environment, FoxP3+ Tregs are capable of expressing T-bet and CXC-chemokine receptor 3 (CXCR3) and produce interferon-γ (IFNγ)[14]. Alternatively, in Th2 environment Tregs can express Blimp-1 and IRF-4, and the chemokine receptors CCR4 and CCR8[15]. Finally, at sites of Th17 inflammation, Tregs which are recruited there express Stat3, retinoic acid receptor- related orphan receptor- γt (RORγt) and CCR6 and produce IL-17. Their ability to respond and adapt depending on the tissue microenvironment raises the possibility that, independently of their plasticity, Tregs may consist of different subsets, characterized by distinct markers and functional properties[16].

Allergic asthma is a major chronic disorder where Tregs have been shown to play a central role in preventing disease development and limiting its severity and exacerbations[17]. Together with related respiratory allergies, it affects more than 300 million people worldwide and ranks as one of the highest socioeconomic burdens among chronic diseases of our century[18,19]. Allergic asthma is characterized by chronic airway inflammation associated with infiltration of immune cells, especially T cells and eosinophils, into the bronchial wall and lumen[20,21]. Elevated serum levels of allergen-specific immunoglobulin (Ig)E, secretion of cytokines and growth factors also characterize the asthmatic phenotype. Activation of Th2 cells orchestrates the inflammatory cascade of the disease, since IL-4 causes isotype switching to IgE, IL-5 promotes the growth and differentiation of eosinophils whilst IL-13 causes airway hyperresponsiveness[22]. As a result, reversible airway obstruction and increased bronchial reactivity develop, leading to breathlessness, wheezing, cough, and chest tightness[23]. This whole process is under the control of FoxP3+ Tregs which accumulate in the lung during allergic airway inflammation, aiming at suppressing effector T cell responses and establishing tolerance to allergens[24,25]. However, it is still unclear which subpopulation(s) confer Tregs their immunoprotective properties, and whether all Tregs are equally capable of suppressing disease.

Here, we addressed this question by comprehensively characterizing the Treg heterogeneity during the development and resolution of allergic airway inflammation using an established model of experimental asthma in mice. We identified a novel FoxP3+ Treg subpopulation, characterized by CD103 expression with elevated immunoregulatory activity that dramatically expands during the resolution phase of the

inflammatory response. CD103$^+$FoxP3$^+$ Tregs express increased levels of immunosuppressive molecules such as ICOS, KLRG1, ENTPD1 (CD39), Gzmb and produce high levels of IL-10 which is prerequisite for their regulatory function. Moreover, we describe novel molecular and mechanistic characteristics of CD103$^+$FoxP3$^+$ Tregs supporting their exploitation therapeutically as strong natural regulators in the context of allergic airway inflammation.

Results

FoxP3$^+$Tregs up-regulate markers of immune suppression and homing during allergic airway inflammation

We hypothesized that populations of Tregs that are specialized to suppress Th2 driven inflammatory responses will exhibit distinct phenotypic and functional characteristics from other Treg populations. To characterize the expression of molecules linked to the suppressive capacity or homing of Tregs, and seek the identification of subpopulations associated with type 2 inflammation, we employed an established mouse model of allergic airway inflammation based on ovalbumin (OVA) sensitization and challenges (Fig. 1A). Inflammation in this model peaks at day 1 post last challenge and gradually declines thereafter, starting to resolve at day 4 and reaching pre-challenge levels of immune cells in the lung at day 10 as previously reported[26].

We used *Foxp3^{egfp}* mice and flow cytometry to analyze the expression of a panel of relevant markers in the lungs and mediastinal lymph nodes (MLNs) during homeostasis (OVA/PBS) or within the resolution phase of inflammation (OVA/OVA). We found that total FoxP3$^+$ T cells, identified as CD45$^+$CD4$^+$FoxP3(gfp)$^+$ from whole lung digest (Fig 1B and S1A) and MLN cells (Fig. 1C and S1B) from OVA/OVA mice upregulated CD44, ICOS, CTLA-4, KLRG1, and CD103 compared to the OVA/PBS group. Interestingly, the highest up-regulated marker was CD103, with more than 3-fold increase in mean fluorescence intensity (MFI) levels observed in the lung of OVA mice (Fig 1B).

We further examined the expression of these markers in the CD103$^+$FoxP3$^+$ Tregs. We observed that CD103 Tregs, identified as CD45$^+$CD4$^+$FoxP3(GFP$^+$)CD103$^+$, are characterized by higher expression of CD127, ICOS, CTLA4, KLRG1 and CD44 compared to their CD103$^-$ counterparts in the OVA/OVA lung (Fig. 1D-E and S1C) and MLNs (Fig. 1D, 1F and S1D). These differences were also present during homeostasis in the CD103$^+$ subpopulation as shown by the expression of these molecules in the PBS-challenged control

mice (Fig. 1D-F and S1C-D). These results indicated that CD103 could be potentially used to discriminate Tregs with high regulatory abilities during allergic airway inflammation.

CD103 marks an increased capacity regulatory T cell population that expands during resolution of allergic airway inflammation

As CD103 has been previously reported to be expressed in a fraction of FoxP3$^+$ Tregs, we examined whether this could also be used to discriminate a distinct regulatory population during the allergic airway inflammation. To explore this hypothesis, we used flow cytometry to characterize the spatiotemporal presence of FoxP3$^+$ Tregs in the lung and the lung-draining MLNs during the initiation, the progression and resolution of the disease (Fig. 2A). Total FoxP3$^+$ cells from whole lungs and MLNs of OVA-challenged and control mice were analyzed via flow cytometry (Fig. S2A). We found that the total number of FoxP3$^+$CD4$^+$ cells significantly increased in the lungs of OVA-challenged mice compared to PBS-challenged control group (Fig. 2B and S2B), despite the unaltered percentages in the MLNs (Fig. 2C and S2C).

Interestingly, we observed that CD103$^+$ Tregs were scarce during homeostasis but they strongly increased following OVA challenge. There was found a 2-fold increase in CD103$^+$FoxP3$^+$CD4$^+$ cells in the lungs of inflamed mice at day 1 post-challenge and they reached the highest expansion during the resolution phase of allergic airway inflammation, on day 4 post last OVA challenge. Surprisingly, more than half of the total FoxP3$^+$ cells expressed CD103 in the lung during the resolution phase of allergic airway inflammation (Fig. 2D and S2B). However, in the MLNs despite the fact that the whole Treg population did not show significant changes, CD103$^+$ Tregs started to infiltrate the LNs after the first challenge with the allergen, peaking at the resolution phase, at day 4 of the protocol (Fig. 2C, 2E and S2C). CD103 marks therefore a subpopulation of FoxP3$^+$ regulatory T cells that increases as the allergic airway inflammation resolves.

CD103$^+$ Tregs reveal a strong regulatory molecular identity

To get insight into the biological involvement of CD103$^+$ Tregs in both homeostasis and allergic airway inflammation, we generated comprehensive RNA-seq gene expression data in CD103+ and CD103$^-$FoxP3$^+$ Tregs isolated from naïve and inflamed lungs. OVA/OVA mice were sacrificed on day 4 of the OVA protocol (Fig. 2A), when the CD103$^+$ reached the highest expansion. CD103$^+$ and CD103$^-$ were collected with cell sorting from total lung extracts of naïve and inflamed tissues. Principal component analysis (PCA) revealed that the CD103 molecule marks a population of Tregs with distinct transcriptional identity (Fig. 3A). Gene-

expression signatures for CD103$^+$ and CD103$^-$ cells in naïve and OVA/OVA lungs were defined by examining differentially expressed genes. CD103$^+$ Tregs exclusively expressed 759 genes under homeostasis and 365 genes during the resolution phase of inflammation, while 228 of them were shared between both conditions when compared to CD103$^-$ Tregs (Fig. 3B).

Next, we analyzed the 20 most significant genes differentially expressed in lung CD103$^+$ Treg population both in naïve and inflammatory conditions. Our results showed that during homeostasis genes encoding the migratory and homing receptors CCR2 and CCR3, the suppression molecules KLRG1 and Gzmb as well as the receptor IL1RL1 (ST2) were among the most significantly upregulated genes in the lung CD103$^+$ Tregs. We also observed that in resting CD103$^+$ Tregs derived from naïve lungs, the transcription factor Tcf7, known for its expression in lymphoid tissue Tregs, and Satb1, an inhibitory gene of the immunosuppressive functions of Tregs, were among the most significantly downregulated genes (Fig. 3C). Of note, during the resolution phase of allergic airway inflammation, the analysis showed that tissue CD103$^+$ Tregs were characterized by high expression of genes encoding the regulatory molecule ICOS and CTLA-2a and the common T cell activation marker IL2Ra (CD25). We also observed that the CD103$^+$ Treg subpopulation in the inflamed lung was able to significantly upregulate the Fgl gene which is necessary for the effective function of Tregs. Furthermore, this cell subset downregulated genes associated with a naïve or central memory phenotype (*Ccr7*, *Sell*). The expression of lymphoid- tissue associated genes *Satb1*, *Bcl2* and *S1pr1* appeared among the most downregulated genes in the inflammatory CD103$^+$ Tregs (Fig. 3C). Collectively, this analysis indicates profound phenotypical and biological differences in CD103$^+$ Tregs in both homeostatic and a Th2 inflammatory environments compared to CD103$^-$ Tregs.

To elucidate the biological role of CD103$^+$ Tregs in a Th2 environment we performed pathway analysis. We found that CD103$^+$ Treg differentially expressed genes are involved in a number of regulatory pathways. So, there is strong evidence that, CD103$^+$ Tregs control inflammatory immune responses especially through negative regulation of T cell activation and proliferation. Pathway analysis also revealed genes involved in cytokine secretion (Fig. 3D and S3A-C).

A heatmap was subsequently generated for a panel of key molecules involved in regulation, homing and activation status of Tregs. Notably, the expression of a number of chemokine receptors including CCR2, CCR4, CCR5, CCR6 and CCR8 was increased in CD103$^+$ Tregs compared to the CD103$^-$ cells. Interestingly, *Ccr7* which is key in driving tissue T cells into draining lymph nodes showed a significant decreased expression pattern in both resting and inflammatory CD103$^+$ Tregs. Moreover, specifically upregulated genes in CD103$^+$ Tregs in the inflamed tissue included *Foxp3*, *Ctla4*, *Gzmb*, *Klrg1*, and *Tigit* which

characterize regulatory T cell subsets with high regulatory capacity. Additionally, $CD103^+$ Tregs from OVA/OVA lungs exhibited up-regulation of the immunoregulatory cytokine IL-10 and a number of transcription factors including MAF, BLIMP-1 (*Prdm1*) and E4BP4 (*Nfil-3*) which are involved in the induction of IL-10 gene expression (Fig. 3E). Overall, these data demonstrate that $CD103^+$ Tregs exhibit a transcriptional profile consistent with increased infiltration into the inflamed tissue and an increased immunoregulatory activity through IL-10 signaling.

$CD103^+$ regulatory T cells exhibit increased suppressive function of Th2 responses correlated with IL-10 production

As our RNAseq data pointed to a notably increased expression of IL-10 in $CD103^+$ Tregs, we wanted to confirm these findings at protein level. We therefore used *$Il10^{egfp}$* reporter mice and analyzed the lungs and MLNs during the resolution phase of allergic airway inflammation (Day 4). The results demonstrated that the $CD103^+$ Tregs, identified as $CD45^+CD4^+CD25^+CD103^+$, produced more IL-10 under inflammatory conditions in the lung and MLNs compared to the negative subset ($CD45^+CD4^+CD25^+CD103^-$). However, these differences appeared milder both in lungs and MLNs of OVA/PBS mice (Fig. 4A-B).

Next, we asked whether these data reflected to an activated functional *in vitro* phenotype in both homeostasis and inflammatory conditions. Thus, we generated RNA-seq data from spleen $CD103^+$ and $CD103^-FoxP3^+$ Tregs isolated from naïve mice. The analysis revealed that $CD103^+$ Tregs have a distinct transcriptional profile compared to the negative population as depicted in the PCA plot (Fig. S4A). We showed that, in homeostasis $CD103^+$ Tregs were characterized by elevated expression of IL-10 and IL-10 related genes (*Maf*, *Prdm1*, *Nfil3*, *Irf4*). Furthermore, we showed that genes such as *Ctla-4*, *Gzm-b*, *Klrg1*, *CD44*, *Tigit* and *Entpd1*, which are known to exert a highly immunosuppressive and immunoregulatory phenotype, were upregulated (Fig. 4C). To unveil the functional properties of the $CD103^+$ subset and further validate the contribution of IL-10 to the regulatory phenotype, we performed co-cultures with effector T cells. We isolated spleen $CD103^+$ and $CD103^-$ Tregs from wild type and *$Il10^{-/-}$* mice and co-cultured them with CFSE- labeled $CD4^+$ T cells according to the protocol (Fig. 4D). Strikingly, the *in vitro* results revealed that $CD103^+$ Tregs had an increased suppressive ability against the proliferation of T cells in culture compared to the $CD103^-$ Treg population ($p<0.05$) (Fig. 4E). However, this feature was lost when Tregs were derived from *$Il10^{-/-}$* mice (Fig. 4E). Therefore, these data suggest an increased modulatory phenotype of $CD103^+$ Tregs in the control of immune responses which depends on the production of IL-10.

CD103^{+} regulatory T cells potently suppress AAI in vivo

To gain an understanding of how these immunoregulatory properties of CD103^{+} Tregs can functionally affect established allergic airway disease and modulate inflammation severity or persistence, we devised a strategy to deplete *in vivo* the CD103^{+} Tregs without affecting the total pool of regulatory T cells. Therefore, we developed *Cd103^{loxp_dtr_loxP} (Cd103^{dtr})* knock-in mice that carry an insertion encoding the human diphtheria toxin receptor–GFP fusion protein (DTR-GFP) preceded by a loxP-flanked transcriptional Stop element under the control of the Cd103 promoter enabling thus a 'two-gene' control of DTR. When crossed with *Foxp3^{cre}*, these mice generated allow the expression of the DTR only in the CD103^{+}FoxP3^{+} cells while sparing the CD103^{-}FoxP3^{+} population (Fig. 5A). This was further validated by PCR which confirmed the presence of *Cre* recombinase and *Egfp*. We also discriminated between the homozygous and heterozygous *Dtr* mice (Fig. S5A-B).

To determine the optimal dose for the most effective deletion of CD103^{+}FoxP3^{+} T cells while minimizing non-specific side effects of the treatment, we injected *Foxp3^{cre}Cd103^{dtr}* mice with several doses (10 ng, 20 ng, 30 ng and 50 ng per gram of body weight) of diphtheria toxin (DT). The lower doses of DT resulted in a modest elimination of the CD103^{+} Treg population from lung and spleen. However, the dose of 50 ng was the most efficient considering that almost two thirds of the total CD103^{+}FoxP3^{+} Treg population were eliminated from the spleen, lung and LNs without affecting the rest of the cell types (Fig. S5C-F).

Using this tool, we next examined the ability of CD103^{+}FoxP3^{+} regulatory T cells to modulate allergic airway inflammation. We treated OVA/OVA mice with DT or PBS post last OVA challenge according to the protocol (Fig. 5B). Surprisingly, we observed that mice lacking CD103^{+}FoxP3^{+} regulatory T cells exhibited lethality, with 70% of the animals dying at day 3 and over 80% by day 4 post challenge (Fig. 5C and S6A). This indicated that loss of CD103^{+} Tregs greatly affects the survival of OVA/OVA mice possibly by altering the local inflammatory milieu, causing pneumonia by damaging the gas-exchange function of the lung.

To test this hypothesis, we injected OVA/OVA *Foxp3^{cre}Cd103^{dtr}* and *Cd103^{dtr}* mice with DT and assessed the inflammatory response on day 2 post last OVA challenge, one day before where cell depletion affects mouse viability (Fig. S6B). Interestingly, we observed that CD103^{+} Treg depletion resulted in markedly increased total leukocyte numbers in the BAL, especially eosinophils and lymphocytes, whereas macrophages and neutrophils were not affected (Fig. 5D-E). Consistently, histological and molecular analysis revealed that CD103^{+} Treg depletion increased peribronchial and perivascular inflammatory cell infiltrates in the lung (Fig. 5F-H and S6C). The higher inflammatory status was also observed by an increase

of specific Th2 responses in MLNs (Fig. 5I). To further explore the regulatory role of $CD103^+$ Tregs in the cytokine production and subsequently in the development of the disease, we performed *in vitro* depletion experiments. According to the protocol, MLNs were collected from asthmatic mice during the resolution of inflammation, at day 4 post last OVA challenge. Both $CD103^+$ and $CD103^-FoxP3^+$ Tregs were isolated from whole LN population with flow cytometry. Then the Treg subsets were re- added in the LN-culture in a dose dependent manner (Fig. S6E). The results showed that the $CD103^+$ subset was able to suppress more effectively the production of IL-5 and IL-13 *in vitro* than the $CD103^-$ population (Fig. 5J). Interestingly, for IFN-γ there was no difference between the two Treg populations.

Most notably, augmented inflammatory response in $CD103^+FoxP3^+$-depleted mice resulted in significantly higher total protein levels and IgM amounts in their BAL compared to control animals indicating increased alveolocapillary membrane permeability, pulmonary edema and damage of the gas exchange function (Fig. 5K-L). Overall, these data reveal a strong regulatory role of $CD103^+$ Treg subpopulation in limiting the Th2-driven inflammation in the lung and controlling allergic airway disease.

Adoptive transfer of $CD103^+$ regulatory T cells potently suppresses allergic airway inflammation

The immunomodulatory activity of $CD103^+$ Treg population in Th2 inflammation prompted us to investigate its potential therapeutic efficacy *in vivo*. To explore whether increased $CD103^+FoxP3^+$ Treg numbers are able to inhibit inflammation and accelerate the resolution phase of allergic airway disease, we carried out adoptive transfer experiments using $CD103^+$ and $CD103^-$ populations in OVA/OVA mice. Wild type mice were sensitized and challenged with OVA according to the protocol. $CD103^+$ and $CD103^-$ $FoxP3^+$ Tregs were isolated using flow cytometry from OVA sensitized *Foxp3*^{egfp} mice and administered i.p prior to the first OVA challenge as indicated in the schematic (Fig. 6A). In this setting, we observed that the transfer of $CD103^+$ population profoundly impacted the disease. Notably, it suppressed the inflammatory cell infiltration in the total BAL numbers and diminished the population of eosinophils and neutrophils compared to the mice that received either the $CD103^-$ Tregs or saline (Fig. 6B-C). These data were also reflected in the histological analysis of the lungs which showed that the $CD103^+$ population decreased the leukocyte infiltration in the inflamed tissue (Fig. 6D). Flow cytometry analysis of lung and MLNs revealed reduced frequencies of $CD4^+$ T cells and DCs in the $CD103^+$ Treg- transferred inflamed mice (Fig. S7A-B). Consistently, the $CD103^+$ Treg administration also decreased OVA-specific Th2 responses in MLNs (IL-5, IL-10 and IL-13) in particular, without altering Th1 cytokines as shown by the IFN-γ levels (Fig. 6E). These findings demonstrate that the exogenous administration of $CD103^+FoxP3^+$ Tregs is capable of

ameliorating allergic airway disease, dampening the Th2-driven inflammatory response in the lung, supporting their potential use for immunotherapeutic purposes.

Discussion

Although, the importance of regulatory T cells for maintaining immune tolerance and homeostasis has been known for decades[27,1], their potential heterogeneity in terms of phenotype and function remains largely unexplored. Our study now identifies a novel population of regulatory T cells, marked by CD103, specialized for restraining Th2-mediated inflammation in the respiratory tract. It demonstrates that $CD103^+FoxP3^+$ Tregs dramatically expand during experimental allergic airway inflammation in mice, reaching over 50% of the total $FoxP3^+$ Treg pool during the resolution phase of the disease, and act to potently suppress Th2 responses while sparing Th1 activity. It further reveals that $CD103^+FoxP3^+$ Tregs constitute a subpopulation of $FoxP3^+$ Tregs with high IL-10 production, exhibiting increased expression of immunosuppressive molecules such as KLRG1, ICOS and Gzmb, and enhanced regulatory activity, and proposes the use of CD103 as a marker for their identification. This sheds light into the functional complexity of $FoxP3^+$ Tregs *in vivo* with important therapeutic implications.

CD103, also termed αEβ7 or ITGAE, is an integrin that can be found on the cell surface of T cells, mostly $CD8^+$ T cells, and dendritic cells (DCs)[28,29]. High frequencies of CD103-expressing cells have been initially described in the gut as their localization in the tissue is facilitated through their binding to e-Cadherin, the natural ligand of CD103[30,31]. This CD103-e-Cadherin interaction has also been proposed to be responsible for the accumulation of CD103-expressing cells to other mucosal sites and tumours[32,33]. Interestingly, previous studies have indicated that CD103 may be a good marker for Tregs with a memory phenotype and may positively influence homing ability to inflamed tissues in order to exert their suppressive functions[34,35]. Moreover, one recent report has shown that CD103 can be used to distinguish effector from regulatory $CD4^+$ T cells in a model of asperillus-induced lung fibrosis, demonstrating that these $CD103^+$ Tregs also express FoxP3 and KLRG1, and play a critical role in limiting disease in this model[36]. Our study therefore expands this current knowledge, showing that CD103 identifies a unique $FoxP3^+$ Treg population with high IL-10 production and potent suppressive activity for Th2 responses and allergic inflammation.

A notable observation made during our studies was the massive increase of $CD103^+FoxP3^+$ Tregs in the lung during the development and resolution phase of allergic airway inflammation. Local expansion and increased migration of $CD103^+FoxP3^+$ Tregs from the periphery or activation and up-regulation of the CD103 marker in $FoxP3^+$ Tregs in the lung may all account for this phenomenon. However, the high

expression of CCR2, CCR4, CCR5, CCR6 and CCR8 in CD103$^+$ FoxP3$^+$ Tregs compared to the CD103$^-$ cells, receptors which promote T cell homing to the lung[37], and the low presence of CCR7 which guides T cells to the draining lymph nodes, indicates that enhanced chemoattraction is part of the process. Expansion of CD103$^+$ FoxP3$^+$ Tregs in the draining lymph nodes and then migration to the inflamed lung is also a strong possibility. Understanding the specifics of this response is key to the development of immunotherapeutic strategies aiming at augmenting regulatory T cell activity in the lung.

Several publications have shown the importance of IL-10 in the immunoregulatory function of FoxP3$^+$ Tregs. FoxP3$^+$ Tregs have the ability to secrete IL-10, a cytokine particularly important in regulating immune responses [38,39,40,41]. Loss of this ability of FoxP3$^+$ Tregs leads to exacerbation allergic inflammation in the lung following intranasal exposure to OVA, characterized by increased IL-5, IL-13 and IFN-γ mRNA levels[40,42]. In the current study, we demonstrate that CD103$^+$FoxP3$^+$ Tregs are the natural producers of IL-10, and therefore the cells largely responsible for IL-10 mediated suppression by Tregs, with CD103$^-$ Tregs been significantly less involved, if at all. Interestingly, high IL-10 production is not the only 'regulatory' characteristic that is augmented in these cells as the expression of KLRG1, ICOS and Gzmb is also enhanced. This points to a coordinated regulatory phenotype induced in these cells that accounts for their function.

Notably, till now it has been difficult to investigate the endogenous function of FoxP3$^+$ Tregs *in vivo* as animal models enabling their specific depletion such as the DEREG mice lead to multi-organ inflammation and death due to the essential role these cells play in keeping whole body homeostasis[5,43]. In addition, depletion of Tregs through administration of the anti-CD25 mAb also reduces activated T helper cells and other non-T cell populations, complicating the interpretation of the data[44,45,46]. In this study, we overcame these problems by developing a novel knock-in mouse permitting the *in vivo* cell-specific deletion of the CD103$^+$FoxP3$^+$ Tregs. This is based on a 'two-gene' approach which allows the expression of DTR in cells that express both gene markers, in this case CD103 and FoxP3, and makes possible the conditional depletion of the CD103$^+$FoxP3$^+$ Treg subset without affecting any other immune cell populations. Strikingly, in our model we reveal that CD103$^+$FoxP3$^+$ Tregs are vital for the survival of mice during the resolution of allergic airway inflammation. The absence of this immunosuppressive population leads to eosinophilic pneumonia and increased alveolocapillary membrane permeability, which causes mortality. Thus, it becomes apparent that loss of CD103$^+$FoxP3$^+$ Tregs alters the local inflammatory milieu leading to damage of the lung gas-exchange function, further highlighting the importance of these cells in maintaining homeostasis in the respiratory tract.

In terms of therapy, drugs such as inhaled corticosteroids can effectively control the asthmatic symptoms[47] but they are unable to change the underlying disease pathophysiology or change its course. Enhancing the Treg activity is thought to be a promising immunotherapeutic strategy to attenuate allergic airway inflammation[48,49]. Adoptive transfer of *in vitro* induced Tregs has been shown to be an effective way to prevent the disease in mouse models of experimental asthma[50,51]. Our study now supports the administration of $CD103^{+}FoxP3^{+}$ cells as a significantly better approach to control allergic airway inflammation compared to the blunt administration of Tregs. This should be of improved efficacy for Th2-driven responses without suppressing non-specifically all T cell immunity and rendering patients susceptible to infections.

In summary, our study uncovers a new highly immunosuppressive subpopulation of regulatory T cells. It also reveals a unique role of these cells in preserving immune homeostasis in the respiratory tract through the selective suppression of Th2 responses and allergic airway inflammation, and advocates for their further exploration in novel therapeutic strategies aiming at treating Th2-mediated inflammatory disorders such as asthma.

Materials and Methods

Mice

Wild-type (WT), *Foxp3*^{egfp}, *Il10*^{egfp}, *Il10*$^{-/-}$, and *Foxp3*^{yfpcre} *(Foxp3*^{cre}*)* mice on a C57BL/6J genetic background were purchased from Jackson Laboratories. The CD103 DTR knock-in mice were made in collaboration with GenOway Transgenic Services (Lyons, France). CD103-DTR knock-in mice were generated by homologous recombination in C57BL/6 embryonic stem cells and maintained on a C57BL/6 background. The targeting construct, assembled by PCR and cloning was generated by the insertion of a loxP-flanked transcription STOP cassette and an IRES DTR/GFP fusion downstream of the long isoform STOP codon located in exon 31. Expression of a DTR-EGFP fusion protein is under the control of the *Cd103* gene in CD103 DTR mice, but is inhibited by a loxp-flanked Stop element. Thus, expression of *Cre* recombinase excises the *Stop* element and allows transcription and translation of DTR-EGFP in cells expressing CD103. For the targeted deletion of $CD103^{+}$ Tregs we crossed the *Cd103*^{dtr} mice with *Foxp3*^{cre} to generate the *Foxp3*^{cre}*Cd103*^{dtr} colony/ strain which allows the ablation of specific Treg population upon DT administration. Genetic screening of *Foxp3*^{cre}*Cd103*^{dtr} mice was carried out by conventional PCR on

genomic DNA from mouse tail biopsies. For the detection of *Cre* recombinase and *Dtr-gfp* the following primers were used respectively: F: AGGATGTGAGGGACTACCTCCTGTA and R: TCCTTCACTCTGATTCTGGCAATTT amplifing a 346 bp fragment and F: CATCTTCTTCAAGGACGAC and R: TTGTGGCTGTTGTAGTTG amplifing a 152bp fragment. To discriminate between homozygous and heterozygous, we performed real time PCR for *Egfp* sequence. All mice were housed and further bred in specific-pathogen free (SPF) conditions in full compliance with FELASA recommendations.

Induction of allergic airway disease

Male mice 6-8 weeks old were sensitized with two intraperitoneal injections of 7.5 μg ovalbumin (OVA, A5503 Sigma) complexed with aluminum hydroxide (AlOH3, Alu-GL-S 12261 Serva). Airway inflammation is induced by three exposures to aerosolized 5% w/v OVA in PBS (OVA/OVA) for 35 min on day -2, -1 and 0 of the protocol. The control mice were sensitized with OVA and challenged with PBS alone(OVA/PBS). The mice were sacrificed at the indicated timepoints for endpoint analysis including inflammatory cell infiltration in the BAL and tissues and OVA-specific mediastinal lymph node responses. All animal studies were approved by the Biomedical Research Foundation, Academy of Athens Ethics Review Board and the local authorities and were in accordance with national and European legislation and guidelines.

Bronchoalveolar lavage and differential cell counts

Bronchoalveolar lavage fluid (BALF) was obtained from whole lung with 0.5ml PBS for two times via a tracheal cannula. Cells were counted using Neubauer chamber and their viability were determined by Trypan blue solution. The cell pellet was subjected onto glass slides using cytospin centrifugation at 600rpm for 3 minutes. Cytospins were stained with May- Grunwald- Giemsa to perform differential cell counts for eosinophils, lymphocytes, neutrophils and monocytes/ macrophages.

Lymph node cultures

Mediastinal lymph nodes were isolated and single-cell suspensions were generated using a 70 μm pore size cell strainer. The cells were cultured at $5x10^5$ cells/well in triplicates in U-shaped 96-well plates in the presence of OVA (100μg/ml). Supernatants were collected after 48h in culture and stored at -20oC for further analysis.

Cytokine measurements

Mouse Th-1 and Th-2 cytokines were quantified in MLN culture supernatants by Sandwich ELISA. ELISA kits were employed for the mouse IL-5 (Biolegend), IL-10 (eBioscience), IL-13 (eBioscience) and IFN-γ (BioLegend).

Isolation of immune cells from lymphoid and non- lymphoid organs

Total lungs were perfused via the right cardiac ventricle with PBS and then immediately harvested. They were cutting into small pieces and digested in 2ml of a solution of collagenase IV and DNase I in PBS containing 1% FBS. The mixture was incubated for 1h at 37oC. The homogenates were passed through a 100μm and then through a 40μm cell strainer and resuspended in PBS containing 1% FBS and 2.5 μM EDTA (FACS buffer). Spleens and LNs were removed and passed through a 70μm cell strainer. The spleen cell suspension was incubated with Red Blood Lysis Buffer to successfully remove the red blood cells. Then the cells were resuspended in FACS Buffer.

Flow cytometry

Single-cell suspensions were pre-incubated with Fc block (2.4G2) to minimize the unspecific staining. Then, 1-2x106 cells were stained with fluorochrome- conjugated antibodies (eBioscience and Biolegend) against surface markers CD3, CD4, CD11c, CD25, CD44, CD45, CD62L, CD103, CD127, CD152 (CTLA-4), CD278 (ICOS), CD304 (Nrp-1), KLRG1, MHCII in PBS containing 1% FBS and 2mM EDTA.

In vitro proliferation assays- CFSE labeling

$CD4^+CD25^+CD103^+$ ($CD103^+$ Tregs) and $CD4^+CD25^+CD103^-$ ($CD103^-$ Tregs) were flow cytometrically sorted from spleen. The sorted Tregs were co-cultured at 1:1 ratio with congenic CFSE-labeled CD4+ T cells isolated with MACS technology from spleen in the presence of 5μg/ml anti-CD3 and 2μg/ml anti-CD28. CFSE-dilution of effector T cells was examined by flow cytometry after four day incubation in culture at 37°C in 5% CO2.

Ex vivo removal of Treg cells from MLN culture

Flow cytometric cell sorting of both $CD4^+FoxP3^+CD103^+$ and $CD4^+FoxP3^+CD103^-$ cells were used to remove the two Treg subsets from MLN single cell suspensions as indicated.

Adoptive transfer

$CD4^+FoxP3^+CD103^+$ and $CD4^+FoxP3^+CD103^-$ Tregs were flow cytometrically sorted from the spleen of OVA sensitized *Foxp3*^{egfp} mice and transferred into wild type mice before the establishment of allergic airway inflammation, prior to the first OVA challenge on day 0 of the protocol by intravenous injections (0.7-1.0x10^5 cells/mice or PBS as control). The mice were sacrificed at the peak of inflammation for endpoint analysis including inflammatory cell infiltration in the BAL, MLNs and lungs as well as OVA-specific MLN responses.

RNA isolation from lungs and qPCR

For gene expression analysis, lungs were collected and immediately snap-frozen in liquid nitrogen. The frozen lungs were homogenized using a tissue homogenizer in TriReagent and RNA isolation was performed through phase separation according to standard protocols. 2 µg of isolated RNA were treated with RQ1 DNAase (Promega) and used for cDNA synthesis with the M-MLV reverse transcriptase (Promega) according to the manufacturer's instructions. Real-time quantitative PCR was performed with iTaq Universal SYBR® Green Supermix (Biorad). Relative amounts of mRNA expression were normalized to Gapdh and calculated according to the $2^{-\Delta\Delta Ct}$ method.

RNA-seq and transcriptomic analysis

For RNA-seq analysis, $CD3^+CD4^+FoxP3^+(gfp^+)CD103^+$ and $CD3^+CD4^+FoxP3^+(gfp^+)CD103^-$ from lung and spleen collected from inflamed and naïve mice were sorted on Aria cell sorter. Total RNA was purified with the RNeasy Micro kit (QIAGEN). RNA samples were treated with DNase I (QIAGEN) and quantified on a NanoDrop (Thermo Scientific). RNA seq libraries were prepared with the TruSeq RNA Library Prep Kit v2 (Illumina) according to the manufacturer's instructions. Quality of the libraries was validated with an Agilent DNA high sensitivity kit run on an Agilent 2100 Bioanalyzer. Bar-coded cDNA libraries were pooled

together in equal concentrations in one pool per biological triplicate or duplicates, and were sequenced on a HiSeq2000 (Illumina) at the Genomics Facility of Biomedical Research Foundation, Academy of Athens.

Bioinformatic tools

The 3D-pca plots were drawn using 'pca3d' package and circular visualization of GO terms was realized using 'GOplot' package, both implemented in R. Volcano plots were constructed using Volcano plot tool at Galaxy Main platform based on ggplot and ggrepel R packages. Heatmaps were drawn using the ComplexHeatmap package in R.

Alveolocapillary membrane permeability measurement

The selective barrier function of the alveolar-capillary membrane is damaged in several lung diseases. This loss of function can be manifested by the leakage of protein-rich fluid from the vascular circulation into the interstitial and/or alveolar spaces. To monitor the alterations in alveolocapillary membrane permeability we measured the total protein concentration in the supernatant of BAL fluid by bicinchoninic acid method (BCA assay) as well as IgM levels by ELISA.

Histological analysis

Lung tissue was isolated, fixed in 10% v/v neutral buffered formalin or 4% PFA:OCT (2:1) and embedded in paraffin or OCT respectively. Slices from paraffin and OCT- embedded lungs were prepared and then stained with hematoxylin and eosin (H&E) for histopathology analysis. The analysis was blindly performed using a semi-quantitative scoring system of infiltrated inflammatory cells. Based on this, both peribronchial and perivascular inflammation were scored giving a maximum score of 8 as previously described *([52,53]).* Histological score for PBS/PBS control mouse lungs was always 0.

Statistical Analysis

Statistical significance of differences ($p < 0.05$) was assessed by Student t test for parametric data and by Mann-Whitney U test for nonparametric data. Data are given as mean values ± SEM.

References

1. Sakaguchi, S. *et al.* Foxp3+CD25+CD4+ natural regulatory T cells in dominant self-tolerance and autoimmune disease. *Immunol. Rev.* **212**, 8–27 (2006).

2. Annacker, O., Burlen-Defranoux, O., Pimenta-Araujo, R., Cumano, A. & Bandeira, A. Regulatory CD4 T Cells Control the Size of the Peripheral Activated/Memory CD4 T Cell Compartment. *J. Immunol.* **164**, 3573–3580 (2000).

3. Gavin, M. A., Clarke, S. R., Negrou, E., Gallegos, A. & Rudensky, A. Homeostasis and anergy of CD4+CD25+ suppressor T cells in vivo. *Nat. Immunol.* **3**, 33–41 (2002).

4. Josefowicz, S. Z., Lu, L.-F. & Rudensky, A. Y. Regulatory T Cells: Mechanisms of Differentiation and Function. *Annu. Rev. Immunol.* **30**, 531–564 (2012).

5. Lahl, K. *et al.* Selective depletion of Foxp3+ regulatory T cells induces a scurfy-like disease. *J. Exp. Med.* **204**, 57–63 (2007).

6. Yamaguchi, T. & Sakaguchi, S. Regulatory T cells in immune surveillance and treatment of cancer. *Semin. Cancer Biol.* **16**, 115–123 (2006).

7. Fontenot, J. D. *et al.* Regulatory T cell lineage specification by the forkhead transcription factor Foxp3. *Immunity* **22**, 329–341 (2005).

8. Bilate, A. M. & Lafaille, J. J. Induced CD4 + Foxp3 + Regulatory T Cells in Immune Tolerance . *Annu. Rev. Immunol.* **30**, 733–758 (2012).

9. Waldmann, H., Adams, E., Fairchild, P. J. & Cobbold, S. Infectious tolerance and the long-term acceptance of transplanted tissue. *Immunol. Rev.* **212**, 301–313 (2006).

10. Fontenot, J. D., Gavin, M. A. & Rudensky, A. Y. Foxp3 programs the development and function of CD4+CD25+ regulatory T cells. *J. Immunol.* **198**, 986–992 (2017).

11. Kim, J. M., Rasmussen, J. P. & Rudensky, A. Y. Regulatory T cells prevent catastrophic autoimmunity throughout the lifespan of mice. *Nat. Immunol.* **8**, 191–197 (2007).

12. Bennett, C. L. *et al.* The immune dysregulation, polyendocrinopathy, enteropathy, X-linked syndrome (IPEX) is caused by mutations of FOXP3. *Nat. Genet.* **27**, 20–21 (2001).

13. Qiu, R. *et al.* Regulatory T Cell Plasticity and Stability and Autoimmune Diseases. *Clin. Rev. Allergy Immunol.* (2018) doi:10.1007/s12016-018-8721-0.

14. Zheng, J. *et al.* Generation of human Th1-like regulatory CD4+ T cells by an intrinsic IFN-γ- and T-bet-dependent pathway. *Eur. J. Immunol.* **41**, 128–139 (2011).

15. Zheng, Y. *et al.* Regulatory T-cell suppressor program co-opts transcription factor IRF4 to control TH2 responses. *Nature* **458**, 351–356 (2009).

16. Burzyn, D., Benoist, C. & Mathis, D. Regulatory T cells in nonlymphoid tissues. *Nat. Immunol.* **14**, 1007–1013 (2013).

17. Ray, A., Khare, A., Krishnamoorthy, N., Qi, Z. & Ray, P. Regulatory T cells in many flavors control asthma. *Mucosal Immunol.* **3**, 216–229 (2010).

18. Soriano, J. B. *et al.* Global, regional, and national deaths, prevalence, disability-adjusted life years, and years lived with disability for chronic obstructive pulmonary disease and asthma, 1990–2015: a systematic analysis for the Global Burden of Disease Study 2015. *Lancet Respir. Med.* **5**, 691–706 (2017).

19. Bahadori, K. *et al.* Economic burden of asthma: A systematic review. *BMC Pulm. Med.* **9**, 1–16 (2009).

20. Robinson, D. S. *et al.* Predominant T H2 -like Bronchoalveolar T-Lymphocyte Population in Atopic Asthma. *N. Engl. J. Med.* **326**, 298–304 (1992).

21. Holgate, S. T. Innate and adaptive immune responses in asthma. *Nat. Med.* **18**, 673–683 (2012).

22. Woodruff, P. G. *et al.* T-helper type 2-driven inflammation defines major subphenotypes of asthma. *Am. J. Respir. Crit. Care Med.* **180**, 388–395 (2009).

23. Jackson, D. J., Sykes, A., Mallia, P. & Johnston, S. L. Asthma exacerbations: Origin, effect, and prevention. *J. Allergy Clin. Immunol.* **128**, 1165–1174 (2011).

24. Kearley, J., Barker, J. E., Robinson, D. S. & Lloyd, C. M. Resolution of airway inflammation and hyperreactivity after in vivo transfer of CD4+CD25+ regulatory T cells is interleukin 10 dependent. *J. Exp. Med.* **202**, 1539–1547 (2005).

25. Chow, Z., Banerjee, A. & Hickey, M. J. Controlling the fire-tissue-specific mechanisms of effector regulatory T-cell homing. *Immunol. Cell Biol.* **93**, 355–363 (2015).

26. Koltsida, O. *et al.* Toll-like receptor 7 stimulates production of specialized pro-resolving lipid mediators and promotes resolution of airway inflammation. *EMBO Mol. Med.* **5**, 762–775 (2013).

27. Sakaguchi, S., Yamaguchi, T., Nomura, T. & Ono, M. Regulatory T Cells and Immune Tolerance. *Cell* **133**, 775–787 (2008).

28. Kilshaw, P. J. & Murant, S. J. A new surface antigen on intraepithelial lymphocytes in the intestine. *Eur. J. Immunol.* **20**, 2201–2207 (1990).

29. Feng, Y. *et al.* CD103 expression is required for destruction of pancreatic islet allografts by CD8+ T cells. *J. Exp. Med.* **196**, 877–886 (2002).

30. Cepek, K. L. *et al.* Adhesion between epithelial cells and T lymphocytes mediated by E-cadherin and the αeβ7 integrin. *Nature* **372**, 190–193 (1994).

31. Schön, M. P. *et al.* Mucosal T lymphocyte numbers are selectively reduced in integrin alpha E (CD103)-deficient mice. *J. Immunol.* **162**, 6641–9 (1999).

32. Anz, D. *et al.* CD103 is a hallmark of tumor-infiltrating regulatory T cells. *Int. J. Cancer* **129**, 2417–2426 (2011).

33. Ruane, D. T. & Lavelle, E. C. The role of CD103+ dendritic cells in the intestinal mucosal immune system. *Front. Immunol.* **2**, 1–6 (2011).

34. Suffia, I., Reckling, S. K., Salay, G. & Belkaid, Y. A Role for CD103 in the Retention of CD4 + CD25 + T reg and Control of Leishmania major Infection . *J. Immunol.* **174**, 5444–5455 (2005).

35. Chen, Z., Herman, A. E., Matos, M., Mathis, D. & Benoist, C. Where CD4+CD25+ T reg cells impinge on autoimmune diabetes. *J. Exp. Med.* **202**, 1387–1397 (2005).

36. Ichikawa, T. *et al.* CD103hi Treg cells constrain lung fibrosis induced by CD103lo tissue-resident

pathogenic CD4 T cells. *Nat. Immunol.* **20**, 1469–1480 (2019).

37. Castan, L., Magnan, A. & Bouchaud, G. Chemokine receptors in allergic diseases. *Allergy Eur. J. Allergy Clin. Immunol.* **72**, 682–690 (2017).

38. Uhlig, H. H. *et al.* Characterization of Foxp3 + CD4 + CD25 + and IL-10-Secreting CD4 + CD25 + T Cells during Cure of Colitis . *J. Immunol.* **177**, 5852–5860 (2006).

39. Maynard, C. L. *et al.* Regulatory T cells expressing interleukin 10 develop from Foxp3+ and Foxp3- precursor cells in the absence of interleukin 10. *Nat. Immunol.* **8**, 931–941 (2007).

40. Rubtsov, Y. P. *et al.* Regulatory T Cell-Derived Interleukin-10 Limits Inflammation at Environmental Interfaces. *Immunity* **28**, 546–558 (2008).

41. Palomares, O., Akdis, M., Martín-Fontecha, M. & Akdis, C. A. Mechanisms of immune regulation in allergic diseases: the role of regulatory T and B cells. *Immunol. Rev.* **278**, 219–236 (2017).

42. Ng, T. H. S. *et al.* Regulation of adaptive immunity; the role of interleukin-10. *Front. Immunol.* **4**, 1–13 (2013).

43. Eji.200939613.pdf, K. & Sparwasser, T. In Vivo Depletion of FoxP3+ Tregs Using the DEREG Mouse Model. in *BioProcess International* vol. 707 157–172 (2011).

44. Setiady, Y. Y., Coccia, J. A. & Park, P. U. In vivo depletion of CD4+FOXP3+ Treg cells by the PC61 anti-CD25 monoclonal antibody is mediated by FcγRIII+ phagocytes. *Eur. J. Immunol.* **40**, 780–786 (2010).

45. Couper, K. N. *et al.* Anti-CD25 Antibody-Mediated Depletion of Effector T Cell Populations Enhances Susceptibility of Mice to Acute but Not Chronic Toxoplasma gondii Infection. *J. Immunol.* **182**, 3985–3994 (2009).

46. Couper, K. N. *et al.* Incomplete Depletion and Rapid Regeneration of Foxp3 + Regulatory T Cells Following Anti-CD25 Treatment in Malaria-Infected Mice . *J. Immunol.* **178**, 4136–4146 (2007).

47. Barnes, P. J. Inhaled corticosteroids. *Pharmaceuticals* **3**, 514–540 (2010).

48. Morita, H. *et al.* An Interleukin-33-Mast Cell-Interleukin-2 Axis Suppresses Papain-Induced Allergic Inflammation By Promoting Regulatory T Cell Numbers. *Immunity* **43**, 175–186 (2015).

49. Palomares, O. *et al.* Regulatory T cells and immune regulation of allergic diseases: Roles of IL-10 and TGF-β. *Genes Immun.* **15**, 511–520 (2014).

50. Xu, W. *et al.* Adoptive transfer of induced-treg cells effectively attenuates murine airway allergic inflammation. *PLoS One* **7**, 1–10 (2012).

51. Joetham, A. *et al.* Inducible and naturally occurring regulatory T cells enhance lung allergic responses through divergent transcriptional pathways. *J. Allergy Clin. Immunol.* **139**, 1331–1342 (2017).

52. Koltsida, O. *et al.* IL-28A (IFN-λ2) modulates lung DC function to promote Th1 immune skewing and suppress allergic airway disease. *EMBO Mol. Med.* **3**, 348–361 (2011).

53. Xirakia, C. *et al.* Toll-like receptor 7-triggered immune response in the lung mediates acute and long-lasting suppression of experimental asthma. *Am. J. Respir. Crit. Care Med.* **181**, 1207–1216 (2010).

Acknowledgments

EA is supported by research grants from the European Commission (IMMUNAID, No 779295), the Hellenic Foundation for Research and Innovation (INTERFLU, No 1574) and Janssen Pharmaceuticals. IEG is supported by a research grant from the Hellenic Foundation for Research and Innovation (RELIEVE, No 506).

Conflict of interest

The authors declare that they have no conflict of interest.

Figure Legends

Fig. 1. CD103 expression markedly increases in FoxP3^{+} regulatory T cells during allergic airway inflammation. **(A)** Experimental protocol of allergic airway inflammation. Male *Foxp3^{gfp}* mice were sensitized with ovalbumin (OVA)-alum and challenged with aerosolized OVA or PBS (control group). Tissue collection was performed at the indicated timepoint. **(B-C)** Expression of CD62L, CD127, NRP1, CD44, ICOS, CTLA-4, KLRG1 and CD103 in total FoxP3^{+} regulatory T cells of asthmatic (OVA) in comparison with the control OVA/PBS lungs **(B)** and LNs **(C)**. **(D)** Representative histogram flow plots comparing the expression of CD127, NRP1, ICOS, CTLA-4 and KLRG1 between CD103^{+} and CD103^{-} Treg cells of both experimental and control lungs and LNs. **(E-F)** Quantification of differential expression of Treg markers between CD103^{+} and CD103^{-} FoxP3^{+} Tregs of and control lungs **(E)** and LNs **(F)**. Data are representative of 4-17 mice per group. One of two representative experiments is shown

Fig. 2. CD103 marks an regulatory T cell population that expands during resolution of AAI. **(A)** Experimental protocol of allergic airway inflammation: male *Foxp3gfp* mice were sensitized with OVA-alum and challenged with aerosolized OVA or PBS. Tissue collection was performed at the indicated timepoints throughout the development, at the peak and the resolution phase of the disease. (**B-C)** Quantification graphs of FoxP3^{+} Tregs from whole lung digests **(B)** and MLNs **(C)** of OVA sensitized, and challenged mice at the indicated time points. **(D-E)** Representative flow plots and quantification graphs of CD103^{+}FoxP3^{+}

subset from whole lung digests **(D)** and MLNs **(E)** of experimental and control mice at the indicated time points. Data are representative of 5-12 mice per group pooled from 3 independent experiments

Fig. 3. CD103 marks a regulatory T cell population with distinct gene expression profile in homeostasis and inflammatory conditions. **(A)** 3D-Principal component analysis (PCA) plot of gene expression data. Dots delimit lung $CD103^+$ and $CD103^-FoxP3^+$ Treg populations in each condition. **(B)** Venn diagram of differentially expressed genes in lung $CD103^+FoxP3^+$ Treg cells in naïve and inflammatory conditions. **(C)** Differentially expressed genes were selected by volcano plots filtering (fold change ≥ 1 and P-value ≤ 0.05). The red and blue points in the plots represent the upregulated and downregulated differentially expressed genes with statistical significance respectively. **(D)** GO analysis of $CD103^+FoxP3^+$ Tregs in OVA/OVA lung. The circles indicate the gene expression distribution in each term, and the z-score of each term indicates the difference in the number of up-regulared versus down-regulated genes divided by the square root of the total count. **(E)** Heatmap of selected differentially expressed genes

Fig. 4. $CD103^+$ regulatory T cells exhibit increased suppressive function in an IL10-dependent manner. **(A-B)** Representative flow plots and graphs of IL-10 expression in $CD103^+$ and CD103- Treg subsets. On day 4 of the protocol, lung **(A)** and LNs **(B)** from OVA/OVA and OVA/PBS *Il10*^{egfp} mice were analyzed with flow cytometry for the expression of IL-10. Data are representative of 4-10 mice per group pooled from 3 independent experiments. **(C)** RNA-seq-based gene expression analysis of spleen $CD103^+$ and $CD103^-$ $FoxP3^+$ T cells isolated from naïve *Foxp3*^{egfp} mice. Heatmap of genes involved in IL-10 signaling and suppression activity of Treg cells in sorted Treg subsets. **(D-E)** *In vitro* suppression assay: Regulatory activity of $CD103^+$ vs $CD103^-$Tregs isolated from wild type and *Il10*$^{-/-}$ mice . CFSE-labeled T responders cells are stimulated together or alone with Tregs **(D)**. Representative histograms show the proliferation of CFSE-labeled $CD4^+$ Tcells which were isolated and cultured according to the protocol **(E)**. Data are pooled from 3 independent experiment.

Fig. 5. $CD103^+$Treg ablation exacerbates allergic airway inflammation in mice. **(A)** Diagrammatic representation of *Foxp3*^{cre}*Cd103*^{dtr} reporter mice. **(B)** Experimental protocol of *in vivo* $CD103^+$ Treg depletion. Male *Foxp3*^{cre}*Cd103*$^{dtr\text{homo}}$ and *Cd103*^{dtr} (control) mice are sensitized with ovalbumin (OVA)-alum and challenged with aerosolized OVA. DT injections are performed post last OVA challenge. The

viability of depleted and non-depleted mice is checked at the indicated timepoints. **(C)** Survival curve in response to treatment of DT. **(D-E)** Total leukocyte numbers **(D)** and differential cell counts for monocytes/macrophages, eosinophils, neutrophils and lymphocytes **(E)** in the BAL at day 2 post DT administration. Levels of leukocytes in healthy controls or saline- challenged animals were <5x104 cells. **(F)** Representative lung sections stained with H&E at day 2 post DT injection. **(G)** Histological assessment of lung inflammation in control and *Cre* mice. **(H)** Molecular expression of cd45 in the lungs of depleted and control mice. **(I)** OVA specific IL-5, IL-10, IL-13 and IFN-γ production in the supernatants of OVA-stimulated MLN cultures at day 2 post DT administration. **(J)** OVA-specific IL-5, IL-10, IL-13 and IFN-γ production in the supernatants of OVA-stimulated MLN cultures at day 4 post-challenge. $CD103^+$ and $CD103^-$ Tregs are isolated from MLN and then are re-added in the culture. Graphs show the production of cytokines when the Treg populations are re-added back to the culture. **(K-L)** Total protein **(K)** and IgM **(L)** concentration in cell- free BAL fluid was determined by BCA assay and ELISA respectively. Data are representative of 4-17 mice per group pooled from 3 independent experiments

Fig. 6. Adoptive transfer of $CD103^+$ Tregs effectively suppress allergic airway inflammation *in vivo*. **(A)** Experimental protocol of adoptive transfer in the development of airway inflammation: C57BL/6 are treated i.v. with $CD103^+FoxP3^+CD4^+$, $CD103^-FoxP3^+CD4^+$ Tregs or PBS before the first challenge with aerosolized OVA. Tissues are collected at the peak of inflammation (day 1). **(B-C)** Total leukocyte counts **(B)** and differential numbers of macrophages (MF), eosinophils (EO), neutrophils (Ne) and lymphocytes (Lymp) **(C)** in the BAL. **(D)** Representative lung sections stained with H&E. **(E)** OVA- specific IL-5, IL-10, IL-13 and IFN-γ production in the supernatants of OVA-stimulated MLN cultures at day 1 post last challenge of Treg or PBS injected mice. Data are representative of 4-17 mice per group pooled from 3 independent experiments

Supplementary Figure Legends

Fig. S1. CD103 expression markedly increases in $FoxP3^+$ regulatory T cells during allergic airway inflammation. Expression of Treg markers in total $FoxP3^+$ regulatory T cells of asthmatic (OVA) in comparison with the control OVA/PBS lungs **(A)** and LNs **(B)**. Representative histogram flow plots and

quantification graphs comparing the expression of CD44 between $CD103^+$ and $CD103^-$ Treg cells of both experimental and control lungs **(C)** and MLNs **(D).**

Fig. S2. CD103 marks an regulatory T cell population that expands during resolution of AAI. **(A)** Flow cytometric gating strategy for total $FoxP3^+$ and $CD103^+$Tregs. **(B-C)** Representative quantification plots of $FoxP3^+$ T cells and $CD103^+FoxP3^+$ T cells as a percentage of total $CD4^+$ T cells in lungs **(B)** and MLNs **(C).**

Fig. S3. CD103 marks a regulatory T cell population with distinct gene expression profile in healthy and inflammatory conditions. **(A)** GO analysis of $CD103^+FoxP3^+$ Tregs in naïve lung. The circles indicate the gene expression distribution in each term, and the z-score of each term indicates the difference in the number of up-regulared versus down-regulated genes divided by the square root of the total count. **(B-C)** Pathway analysis of genes differentially expressed in $CD103^+$ Tregs compares to $CD103^-$ Tregs isolated from lungs of naïve **(B)** and OVA/OVA **(C)** *Foxp3*^{gfp} mice.

Fig. S4. $CD103^+$ regulatory T cells exhibit increased suppressive function in an IL-10-dependent manner. **(A)** 3D-PCA plot of gene expression data. Dots delimit spleen $CD103^+$ and $CD103^-FoxP3^+$ Treg populations of naïve *Foxp3*^{egfp} mice. **(B)** Pathway analysis of genes differentially expressed in $CD103^+$Tregs compares to $CD103^-$Tregs isolated from spleen of naïve *Foxp3*^{egfp} mice.

Fig. S5. Validation of *Foxp3*^{cre}*Cd103*^{dtr} mouse. **(A)** Presence of the targeted allele in *Foxp3*^{cre}*Cd103*^{dtr} mice determined by conventional PCR. **(B)** Heterozygous from homozygous genotypes of *Foxp3*^{cre}*Cd103*^{dtr} mice distinguished by qPCR against *Egfp*. **(C)** Representative flow cytometry plots of $CD103^+FoxP3^+$ T cells in spleenocytes and lung digests after dose dependently administration of DT. **(D-E)** Quantification of $CD103^+$ Treg cells and $CD103^+$ non Tregs cells in spleenocytes **(D)** and lung digest **(E)** 24h post administration of DT. **(F)** Representative quantification graphs of CD103+ Tregs cells in spleenocytes, LN cell suspension and lung digest 24h post administration of 50ng/mousegr DT.

Fig. S6. $CD103^+$Treg ablation exacerbates allergic airway inflammation in mice. **(A)** Survival curve in response to treatment of DT. **(B)** Experimental protocol of *in vivo* $CD103^+$Treg depletion. Male

Foxp3^{cre}*Cd103*^{dtrhomo} and *Cd103*^{dtr} (control) mice are sensitized with ovalbumin (OVA)-alum and challenged with aerosolized OVA. DT injections are performed post last OVA challenge. The mice are sacrificed for endpoint analysis. **(C)** Representative lung sections stained with H&E. **(D)** Il5, Il13, Ifnγ and Bcl2 expression in lungs. **(E)** Experimental protocol for *in vitro* culture: CD103^{+} and CD103^{-} Tregs are isolated from MLNs of day 4 OVA/OVA *Foxp3*^{egfp} mice. Then rest LN cell suspension are cultured in the presence of OVA and both population of Treg are re-added in a dose dependent manner.

Fig. S7. Adoptive transfer of CD103^{+} Tregs effectively suppress allergic airway inflammation *in vivo*. T cell and DC percentages in lung digests **(A)** and MLNs **(B)**.

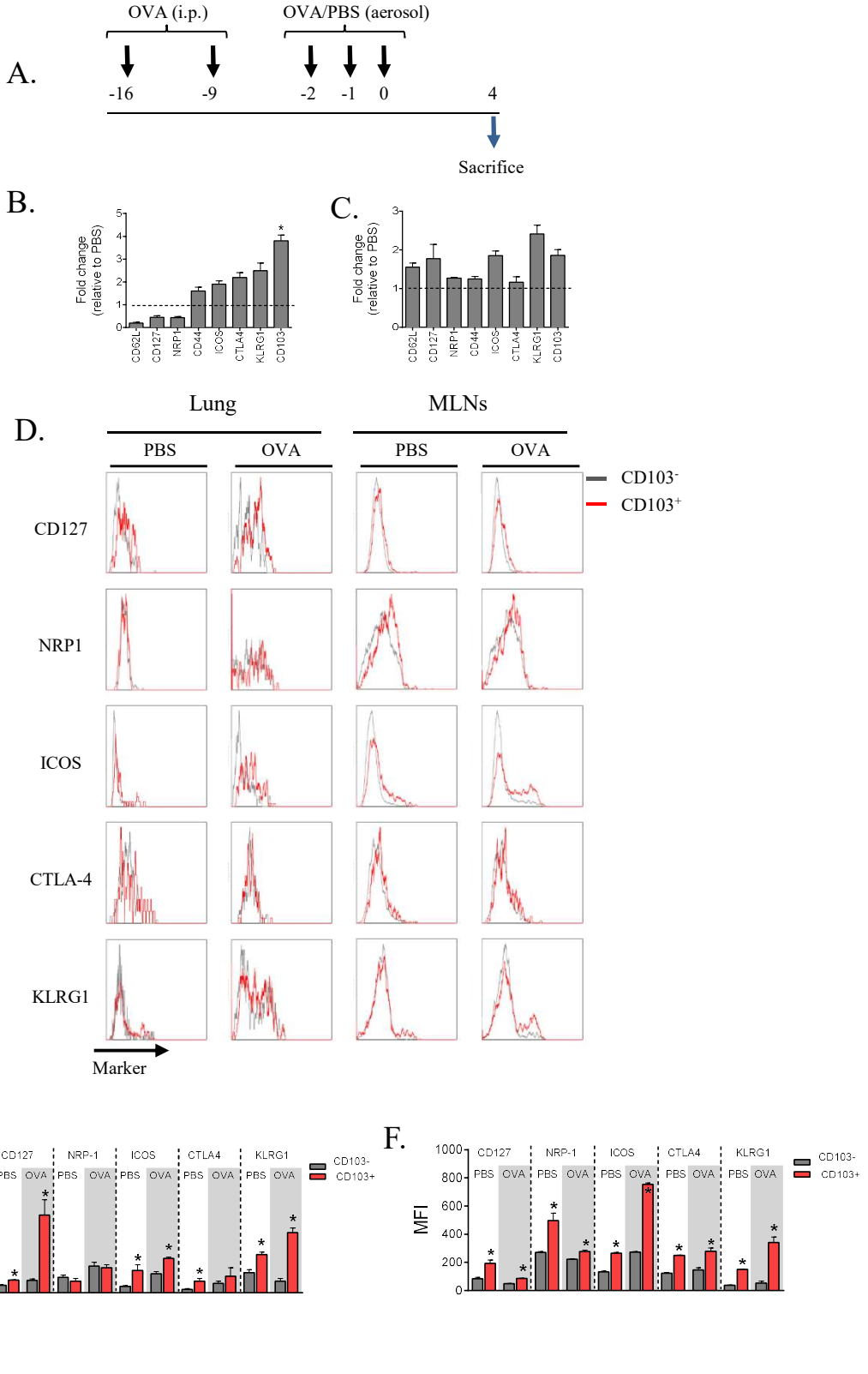
A.
OVA (i.p.)
OVA/PBS (aerosol)
-16
-9
-2
-1
0
4
Sacrifice
B.
Fold change (relative to PBS)
CD62L
CD127
NRP1
CD44
ICOS
CTLA4
KLRG1
CD103
C.
Fold change (relative to PBS)
D.
Lung
MLNs
PBS
OVA
CD103-
CD103+
CD127
NRP1
ICOS
CTLA-4
KLRG1
Marker
E.
MFI
F.
MFI

FIG. 1

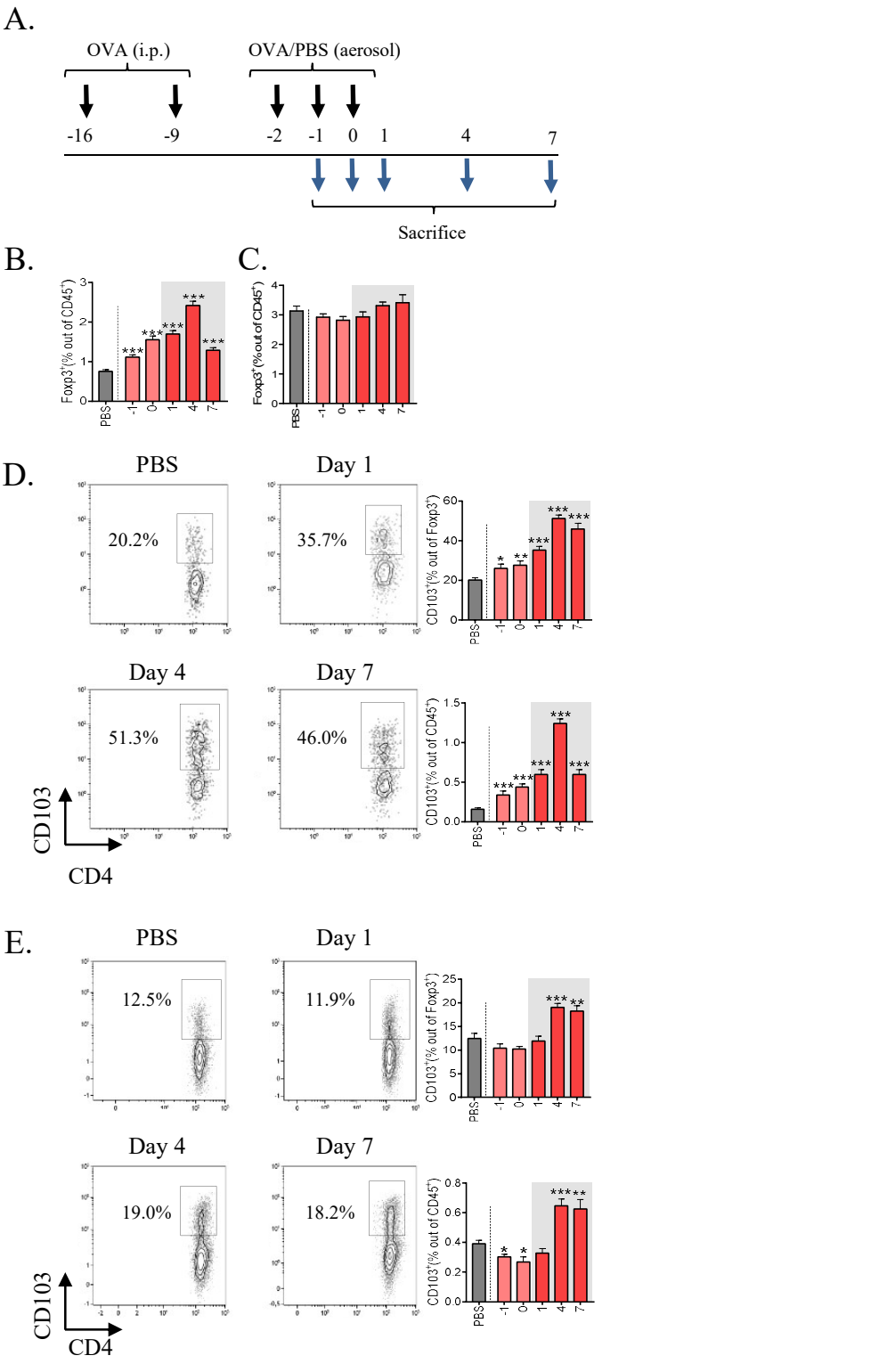
A.
OVA (i.p.)
OVA/PBS (aerosol)
-16
-9
-2
-1
0
1
4
7
Sacrifice
B.
C.
Foxp3+(% out of CD45+)
PBS
-1
0
1
4
7
D.
PBS
Day 1
Day 4
Day 7
20.2%
35.7%
51.3%
46.0%
CD103+(% out of Foxp3+)
CD103+(% out of CD45+)
CD103
CD4
E.
12.5%
11.9%
19.0%
18.2%

FIG. 2

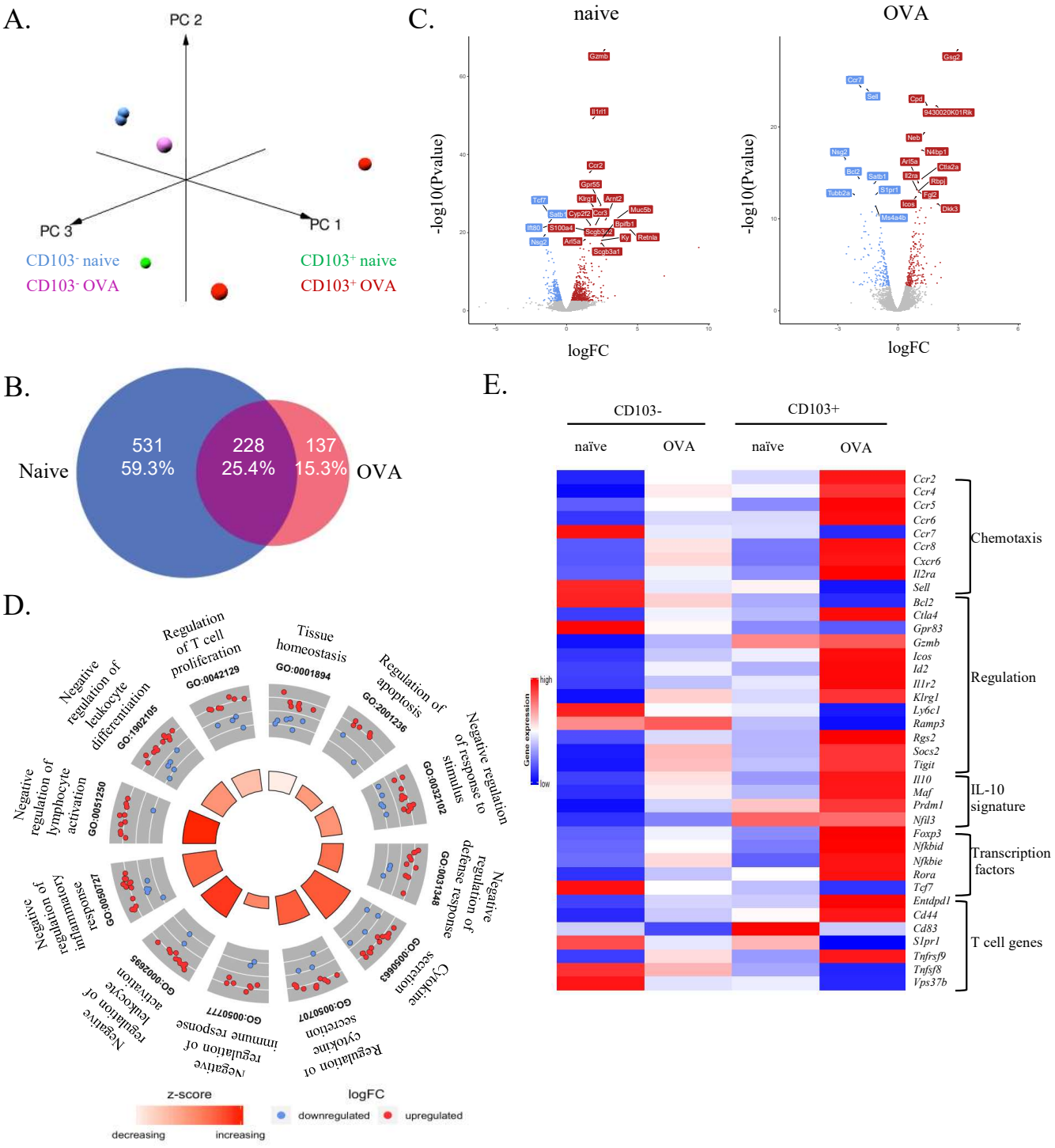
A.
PC 2
PC 3
PC 1
CD103- naive
CD103+ naive
CD103- OVA
CD103+ OVA
B.
Naive
531
59.3%
228
25.4%
137
15.3%
OVA
C.
naive
OVA
-log10(Pvalue)
logFC
Gzmb
Il1r1
Ccr2
Gpr55
Tcf7
Klrg1
Arnt2
Muc5b
Saltb
Cyp2f2
Ccr3
Ifit80
S100a4
Bpifb1
Scgb3a2
Ky
Retnla
Nsg2
Arl5a
Scgb3a1
Gsg2
Ccr7
Sell
Cpd
9430020K01Rik
Neb
Nsg2
N4bp1
Arl5a
Bcl2
Ctla2a
Il2ra
Rbpj
Satb1
Tubb2a
S1pr1
Fgl2
Icos
Dkk3
Ms4a4b
D.
Regulation of T cell proliferation
GO:0042129
Tissue homeostasis
GO:0001894
Regulation of apoptosis
GO:2001236
Negative regulation of response to stimulus
GO:0032102
Negative regulation of defense response
GO:0031348
Cytokine secretion
GO:0050663
Regulation of cytokine secretion
GO:0050707
Negative regulation of immune response
GO:0050777
Negative regulation of leukocyte activation
GO:0002695
Negative regulation of inflammatory response
GO:0090727
Negative regulation of lymphocyte activation
GO:0051250
Negative regulation of leukocyte differentiation
GO:1902105
z-score
decreasing
increasing
logFC
downregulated
upregulated
E.
CD103-
CD103+
naïve
OVA
naïve
OVA
Gene expression
high
low
Ccr2
Ccr4
Ccr5
Ccr6
Ccr7
Ccr8
Cxcr6
Il2ra
Sell
Bcl2
Ctla4
Gpr83
Gzmb
Icos
Id2
Il1r2
Klrg1
Ly6c1
Ramp3
Rgs2
Socs2
Tigit
Il10
Maf
Prdm1
Nfil3
Foxp3
Nfkbid
Nfkbie
Rora
Tcf7
Entdpd1
Cd44
Cd83
S1pr1
Tnfrsf9
Tnfsf8
Vps37b
Chemotaxis
Regulation
IL-10 signature
Transcription factors
T cell genes

FIG. 3

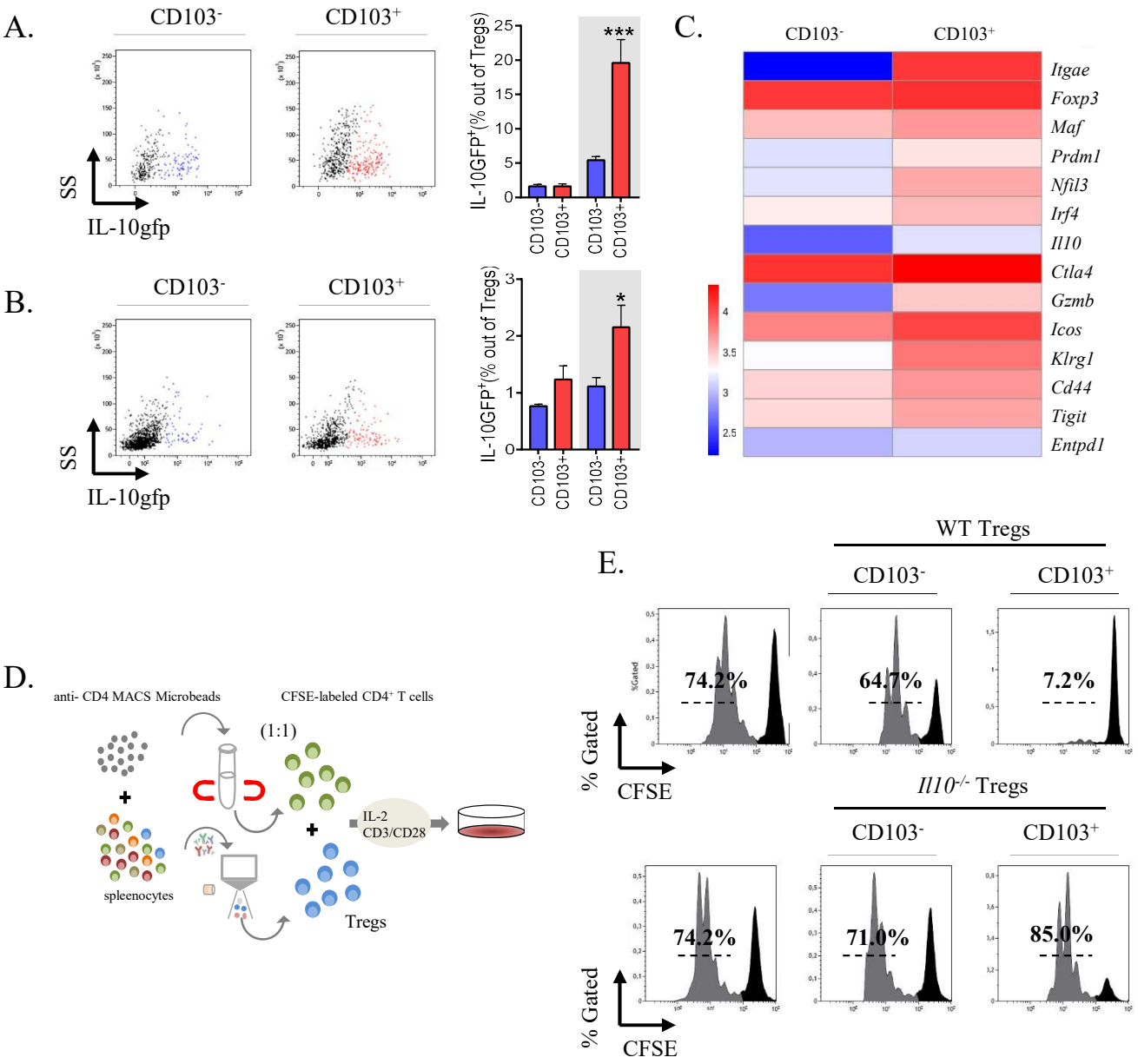
A.
CD103-
CD103+
SS
IL-10gfp
IL-10GFP+(% out of Tregs)
***
CD103-
CD103+
CD103-
CD103+
B.
CD103-
CD103+
SS
IL-10gfp
IL-10GFP+(% out of Tregs)
*
CD103-
CD103+
CD103-
CD103+
C.
CD103-
CD103+
Itgae
Foxp3
Maf
Prdm1
Nfil3
Irf4
Il10
Ctla4
Gzmb
Icos
Klrg1
Cd44
Tigit
Entpd1
4
3.5
3
2.5
D.
anti- CD4 MACS Microbeads
CFSE-labeled CD4+ T cells
(1:1)
IL-2
CD3/CD28
spleenocytes
Tregs
E.
WT Tregs
CD103-
CD103+
74.2%
64.7%
7.2%
% Gated
CFSE
Il10-/- Tregs
CD103-
CD103+
74.2%
71.0%
85.0%
% Gated
CFSE

FIG. 4

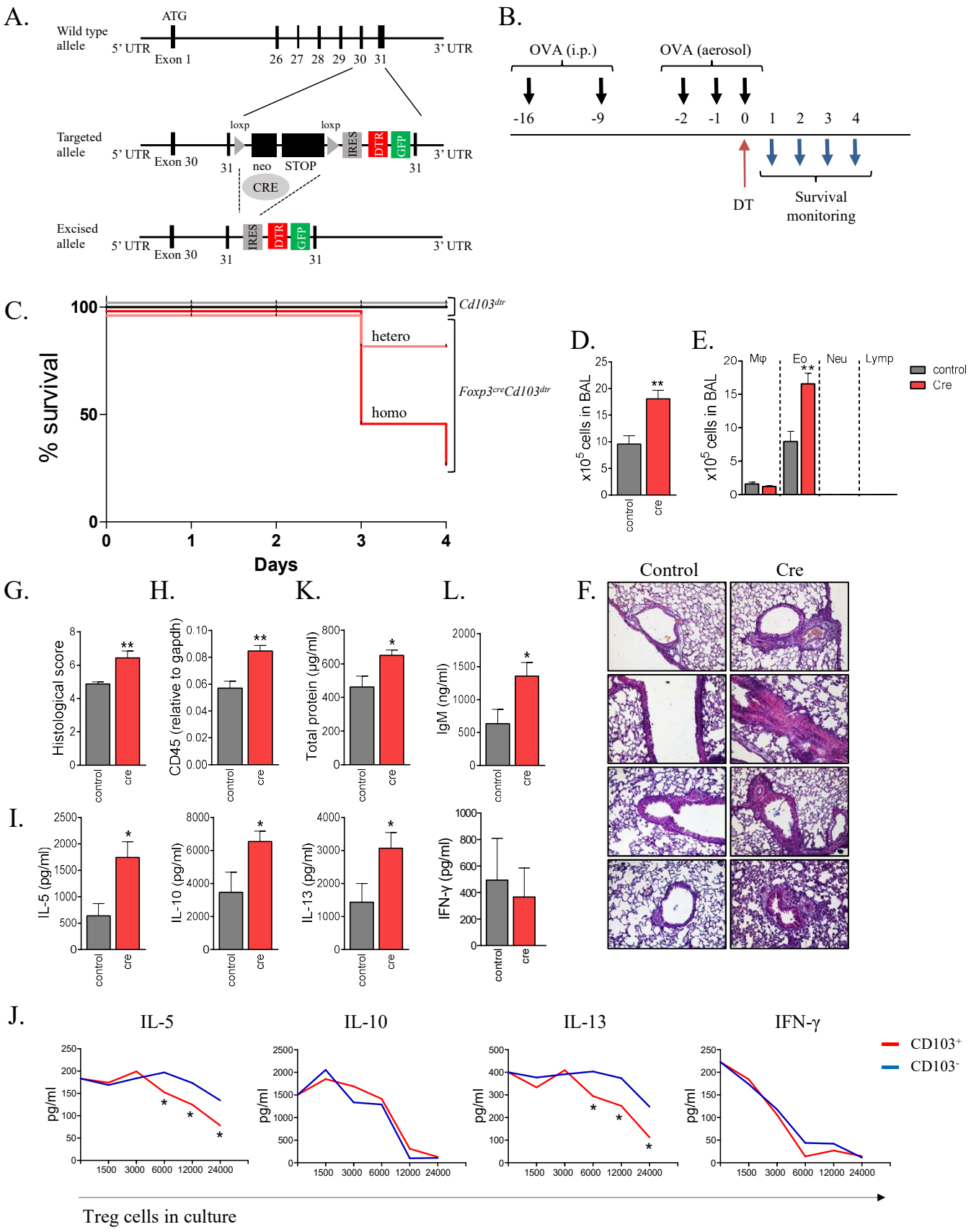
A.
Wild type allele
ATG
5' UTR
Exon 1
26 27 28 29 30 31
3' UTR
Targeted allele
loxp
loxp
IRES
DTR
GFP
neo
STOP
CRE
Excised allele
B.
OVA (i.p.)
OVA (aerosol)
-16
-9
-2
-1
0
1
2
3
4
DT
Survival monitoring
C.
% survival
Days
Cd103dtr
Foxp3creCd103dtr
hetero
homo
D.
x10^5 cells in BAL
control
cre
E.
Mφ
Eo
Neu
Lymp
control
Cre
F.
Control
Cre
G.
Histological score
H.
CD45 (relative to gapdh)
K.
Total protein (μg/ml)
L.
IgM (ng/ml)
I.
IL-5 (pg/ml)
IL-10 (pg/ml)
IL-13 (pg/ml)
IFN-γ (pg/ml)
J.
IL-5
IL-10
IL-13
IFN-γ
pg/ml
CD103+
CD103-
Treg cells in culture

FIG. 5

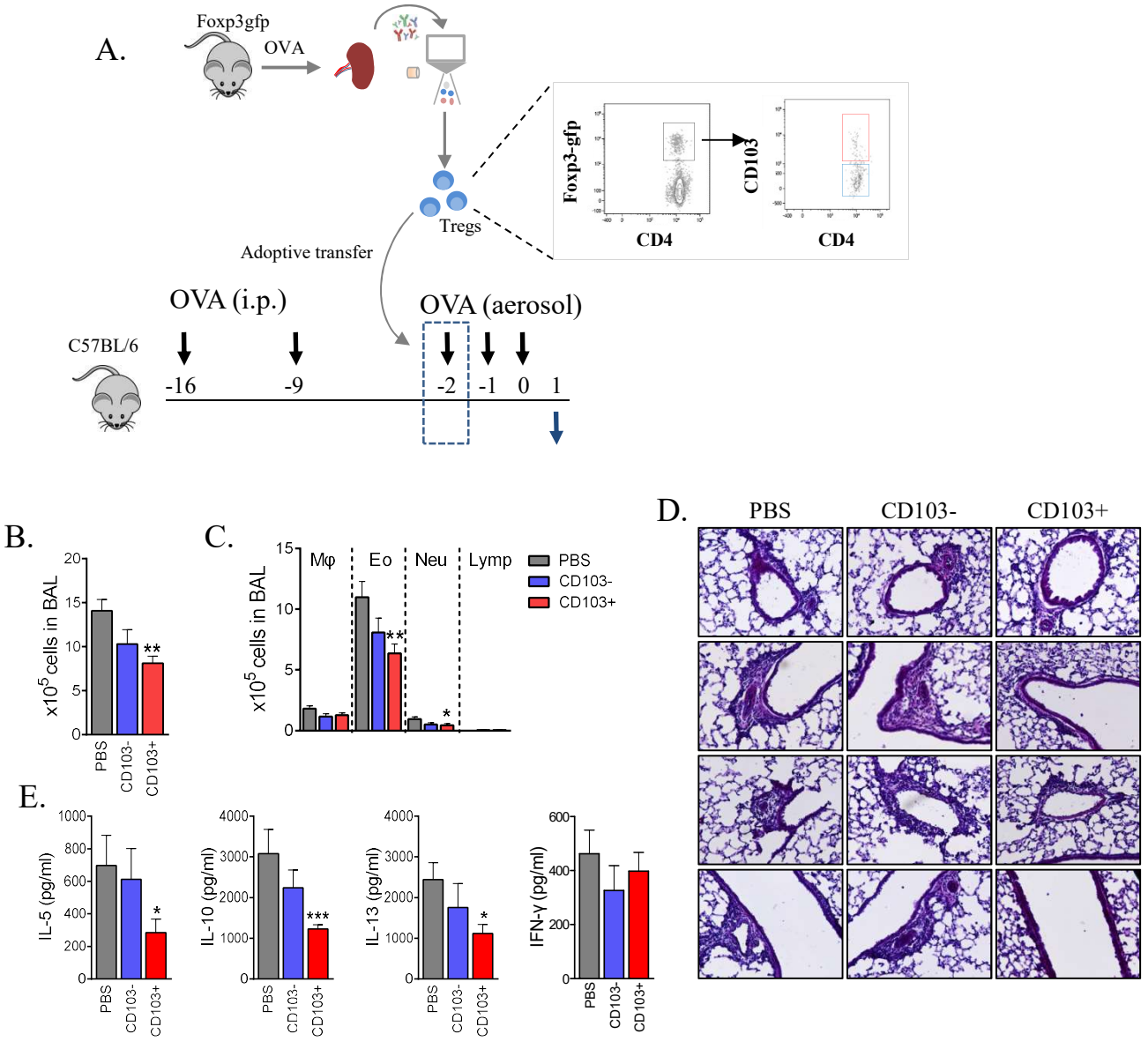
A.
Foxp3gfp
OVA
Tregs
Foxp3-gfp
CD4
CD103
CD4
Adoptive transfer
OVA (i.p.)
OVA (aerosol)
C57BL/6
-16
-9
-2
-1
0
1
B.
x10^5 cells in BAL
PBS
CD103-
CD103+
C.
Mφ
Eo
Neu
Lymp
PBS
CD103-
CD103+
x10^5 cells in BAL
D.
PBS
CD103-
CD103+
E.
IL-5 (pg/ml)
IL-10 (pg/ml)
IL-13 (pg/ml)
IFN-γ (pg/ml)

FIG. 6

Supplementary Figures

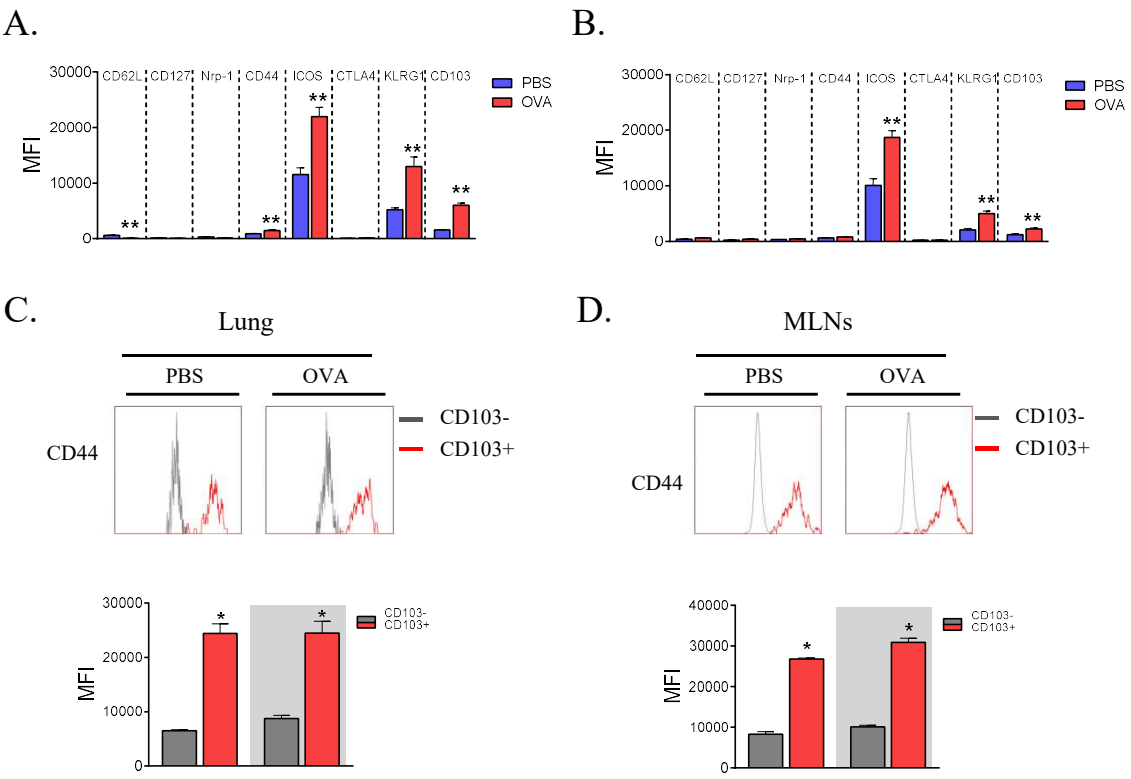
A.
B.
C.
D.
Lung
MLNs
PBS
OVA
CD62L
CD127
Nrp-1
CD44
ICOS
CTLA4
KLRG1
CD103
MFI
CD103-
CD103+

Fig. S1

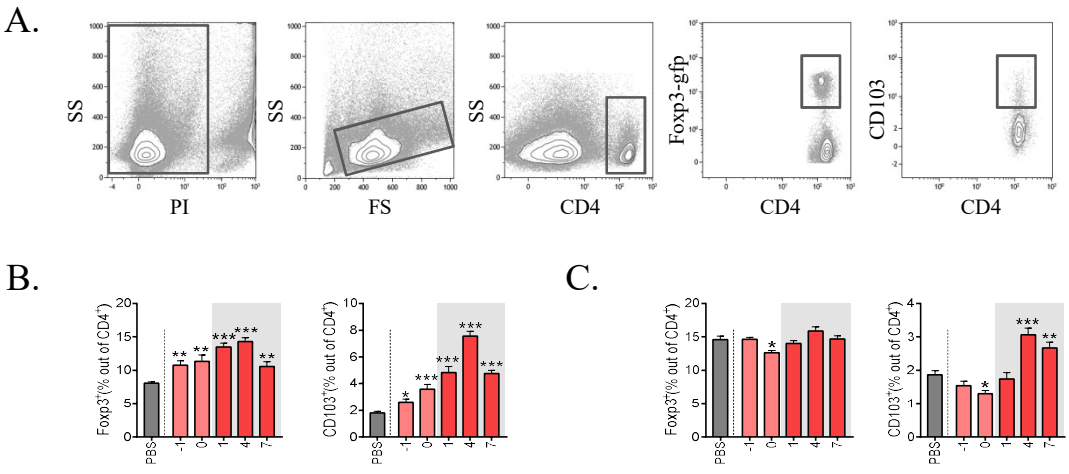
A.
SS
PI
SS
FS
SS
CD4
Foxp3-gfp
CD4
CD103
CD4
B.
Foxp3+(% out of CD4+)
CD103+(% out of CD4+)
PBS
-1
0
1
4
7
C.
Foxp3+(% out of CD4+)
CD103+(% out of CD4+)
PBS
-1
0
1
4
7

Fig. S2

A.

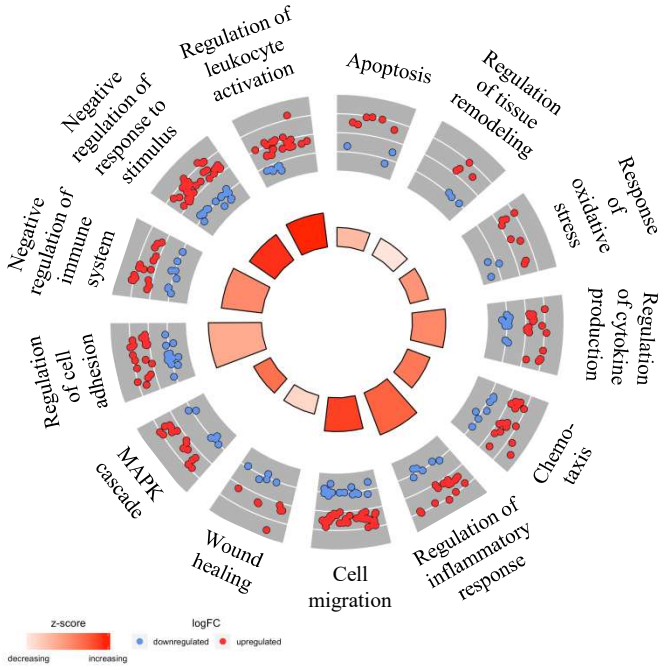
Regulation of leukocyte activation
Apoptosis
Regulation of tissue remodeling
Response of oxidative stress
Regulation of cytokine production
Chemo-taxis
Regulation of inflammatory response
Cell migration
Wound healing
MAPK cascade
Regulation of cell adhesion
Negative regulation of immune system
Negative regulation of response to stimulus
z-score
decreasing
increasing
logFC
downregulated
upregulated

B.

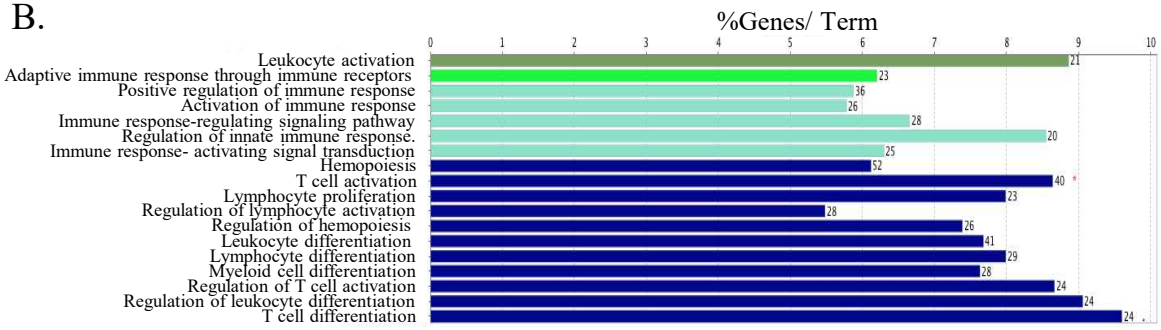
%Genes/ Term
Leukocyte activation
Adaptive immune response through immune receptors
Positive regulation of immune response
Activation of immune response
Immune response-regulating signaling pathway
Regulation of innate immune response.
Immune response- activating signal transduction
Hemopoiesis
T cell activation
Lymphocyte proliferation
Regulation of lymphocyte activation
Regulation of hemopoiesis
Leukocyte differentiation
Lymphocyte differentiation
Myeloid cell differentiation
Regulation of T cell activation
Regulation of leukocyte differentiation
T cell differentiation

C.

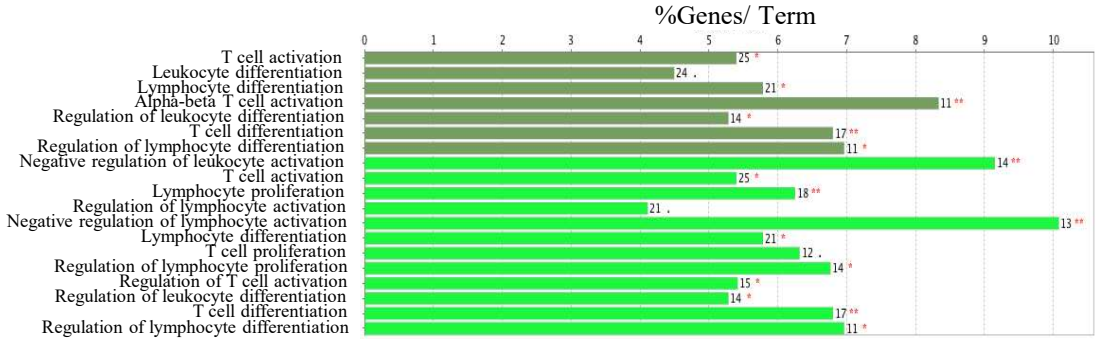
%Genes/ Term
T cell activation
Leukocyte differentiation
Lymphocyte differentiation
Alpha-beta T cell activation
Regulation of leukocyte differentiation
T cell differentiation
Regulation of lymphocyte differentiation
Negative regulation of leukocyte activation
T cell activation
Lymphocyte proliferation
Regulation of lymphocyte activation
Negative regulation of lymphocyte activation
Lymphocyte differentiation
T cell proliferation
Regulation of lymphocyte proliferation
Regulation of T cell activation
Regulation of leukocyte differentiation
T cell differentiation
Regulation of lymphocyte differentiation

Fig. S3

A.

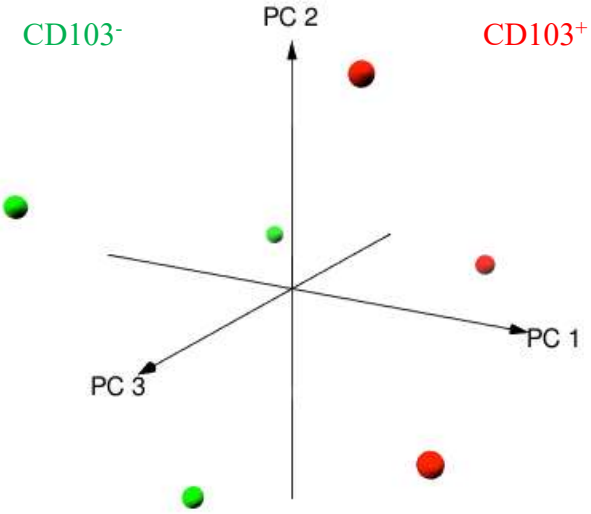
CD103-
CD103+
PC 2
PC 1
PC 3

B.

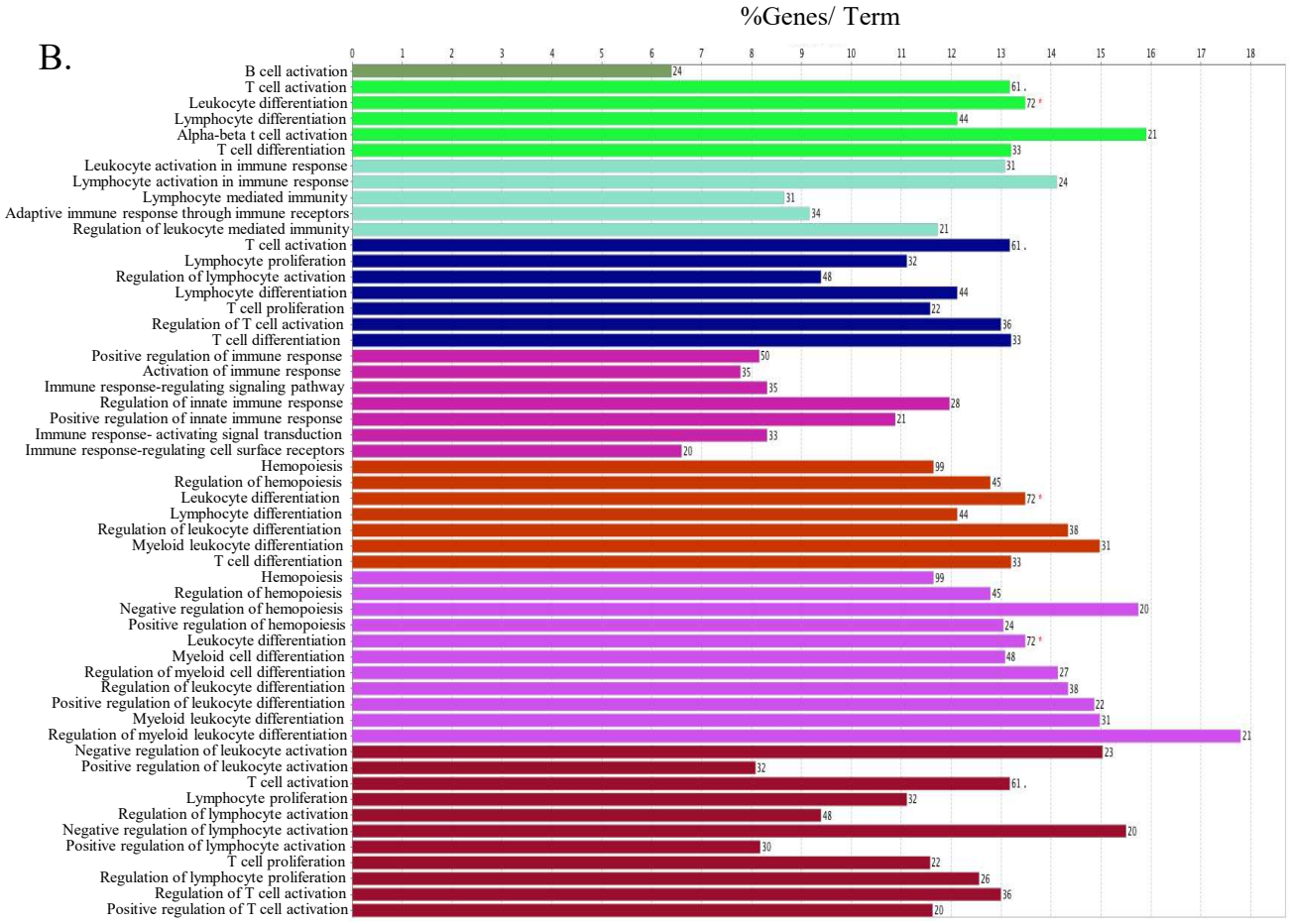
%Genes/ Term
0 1 2 3 4 5 6 7 8 9 10 11 12 13 14 15 16 17 18
B cell activation 24
T cell activation 61
Leukocyte differentiation 72
Lymphocyte differentiation 44
Alpha-beta t cell activation 21
T cell differentiation 33
Leukocyte activation in immune response 31
Lymphocyte activation in immune response 24
Lymphocyte mediated immunity 31
Adaptive immune response through immune receptors 34
Regulation of leukocyte mediated immunity 21
T cell activation 61
Lymphocyte proliferation 32
Regulation of lymphocyte activation 48
Lymphocyte differentiation 44
T cell proliferation 22
Regulation of T cell activation 36
T cell differentiation 33
Positive regulation of immune response 50
Activation of immune response 35
Immune response-regulating signaling pathway 35
Regulation of innate immune response 28
Positive regulation of innate immune response 21
Immune response- activating signal transduction 33
Immune response-regulating cell surface receptors 20
Hemopoiesis 99
Regulation of hemopoiesis 45
Leukocyte differentiation 72
Lymphocyte differentiation 44
Regulation of leukocyte differentiation 38
Myeloid leukocyte differentiation 31
T cell differentiation 33
Hemopoiesis 99
Regulation of hemopoiesis 45
Negative regulation of hemopoiesis 20
Positive regulation of hemopoiesis 24
Leukocyte differentiation 72
Myeloid cell differentiation 48
Regulation of myeloid cell differentiation 27
Regulation of leukocyte differentiation 38
Positive regulation of leukocyte differentiation 22
Myeloid leukocyte differentiation 31
Regulation of myeloid leukocyte differentiation 21
Negative regulation of leukocyte activation 23
Positive regulation of leukocyte activation 32
T cell activation 61
Lymphocyte proliferation 32
Regulation of lymphocyte activation 48
Negative regulation of lymphocyte activation 20
Positive regulation of lymphocyte activation 30
T cell proliferation 22
Regulation of lymphocyte proliferation 26
Regulation of T cell activation 36
Positive regulation of T cell activation 20

Fig. S4

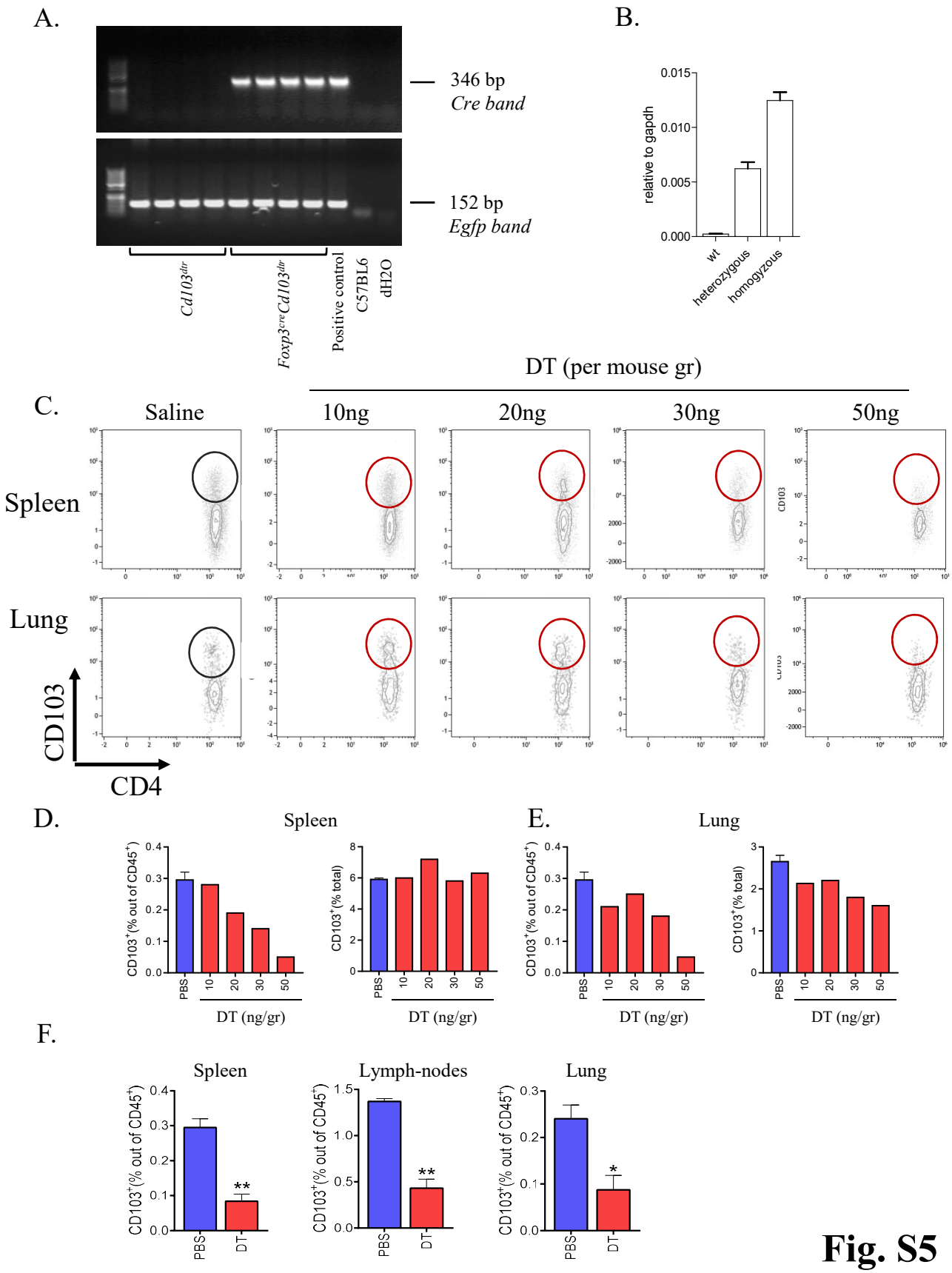
A.
346 bp
Cre band
152 bp
Egfp band
Cd103dtr
Foxp3creCd103dtr
Positive control
C57BL6
dH2O
B.
relative to gapdh
0.015
0.010
0.005
0.000
wt
heterozygous
homogyzous
DT (per mouse gr)
C.
Saline
10ng
20ng
30ng
50ng
Spleen
Lung
CD103
CD4
D.
Spleen
CD103+(% out of CD45+)
CD103+(% total)
PBS
10
20
30
50
DT (ng/gr)
E.
Lung
F.
Spleen
Lymph-nodes
Lung
PBS
DT
**
*

Fig. S5

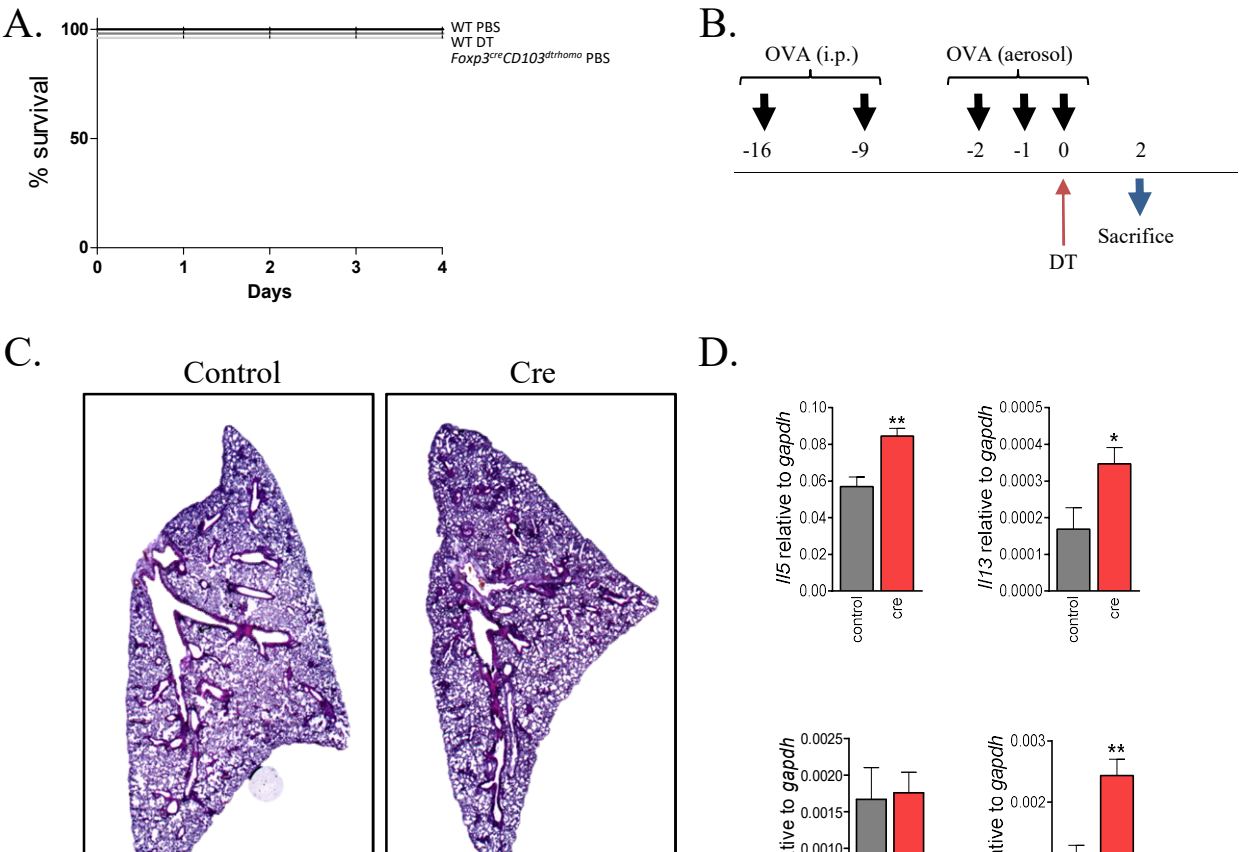
A.
100
50
0
% survival
0
1
2
3
4
Days
WT PBS
WT DT
Foxp3cre CD103dtrhomo PBS
B.
OVA (i.p.)
OVA (aerosol)
-16
-9
-2
-1
0
2
DT
Sacrifice
C.
Control
Cre
D.
Il5 relative to gapdh
Il13 relative to gapdh
Ifnγ relative to gapdh
Bcl2 relative to gapdh
control
cre
E.
Foxp3gfp
+ OVA
Tregs

Fig. S6

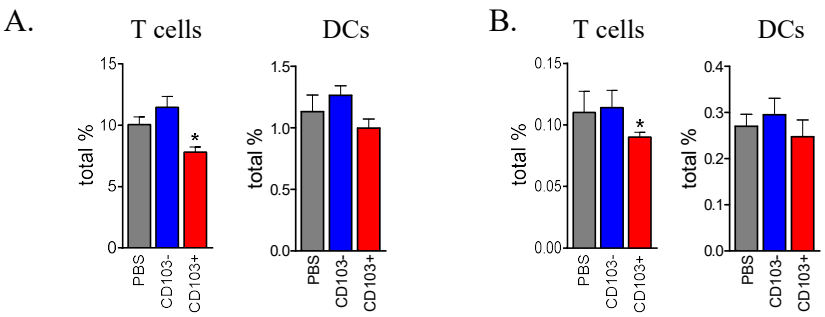
A.
T cells
DCs
total %
15
10
5
0
1.5
1.0
0.5
0.0
*
PBS
CD103-
CD103+
B.
T cells
DCs
total %
0.15
0.10
0.05
0.00
0.4
0.3
0.2
0.1
0.0
*
PBS
CD103-
CD103+

Fig. S7